



OPEN ACCESS

EDITED BY

Hui Ni,
Jimei University,
China

REVIEWED BY

Santosh Kumar Tiwari,
Maharshi Dayanand University,
India
Hsin Chih Lai,
Chang Gung University,
Taiwan

*CORRESPONDENCE

Xiaoyan Wang
wxy220011@163.com

SPECIALTY SECTION

This article was submitted to
Food Microbiology,
a section of the journal
Frontiers in Microbiology

RECEIVED 19 June 2022
ACCEPTED 05 August 2022
PUBLISHED 08 September 2022

CITATION

Zhang C, Ma K, Nie K, Deng M, Luo W, Wu X, Huang Y and Wang X (2022)
Assessment of the safety and probiotic properties of *Roseburia intestinalis*: A potential "Next Generation Probiotic".
Front. Microbiol. 13:973046.
doi: 10.3389/fmicb.2022.973046

COPYRIGHT

© 2022 Zhang, Ma, Nie, Deng, Luo, Wu, Huang and Wang. This is an open-access article distributed under the terms of the Creative Commons Attribution License (CC BY). The use, distribution or reproduction in other forums is permitted, provided the original author(s) and the copyright owner(s) are credited and that the original publication in this journal is cited, in accordance with accepted academic practice. No use, distribution or reproduction is permitted which does not comply with these terms.

Assessment of the safety and probiotic properties of *Roseburia intestinalis*: A potential "Next Generation Probiotic"

Chao Zhang¹, Kejia Ma¹, Kai Nie¹, Minzi Deng¹, Weiwei Luo¹,
Xing Wu¹, Yujun Huang¹ and Xiaoyan Wang^{1,2*}

¹Department of Gastroenterology, The Third Xiangya Hospital of Central South University, Changsha, China, ²Hunan Key Laboratory of Nonresolving Inflammation and Cancer, Cancer Research Institute, Central South University, Changsha, China

Roseburia intestinalis is an anaerobic bacterium that produces butyric acid and belongs to the phylum Firmicutes. There is increasing evidence that this bacterium has positive effects on several diseases, including inflammatory bowel disease, atherosclerosis, alcoholic fatty liver, colorectal cancer, and metabolic syndrome, making it a potential "Next Generation Probiotic." We investigated the genomic characteristics, probiotic properties, cytotoxicity, oral toxicity, colonization characteristics of the bacterium, and its effect on the gut microbiota. The genome contains few genes encoding virulence factors, three clustered regularly interspaced short palindromic repeat (CRISPR) sequences, two Cas genes, no toxic biogenic amine synthesis genes, and several essential amino acid and vitamin synthesis genes. Seven prophages and 41 genomic islands were predicted. In addition to a bacteriocin (Zoocin A), the bacterium encodes four metabolic gene clusters that synthesize short-chain fatty acids and 222 carbohydrate-active enzyme modules. This bacterium is sensitive to antibiotics specified by the European Food Safety Authority, does not exhibit hemolytic or gelatinase activity, and exhibits some acid resistance. *R. intestinalis* adheres to intestinal epithelial cells and inhibits the invasion of certain pathogens. *In vitro* experiments showed that the bacterium was not cytotoxic. *R. intestinalis* did not affect the diversity or abundance of the gut flora. Using the fluorescent labelling method, we discovered that *R. intestinalis* colonizes the cecum and mucus of the colon. An oral toxicity study did not reveal any obvious adverse effects. The lethal dose (LD₅₀) of *R. intestinalis* exceeded 1.9×10^9 colony forming units (CFU)/kg, whereas the no observed adverse effect level (NOAEL) derived from this study was 1.32×10^9 CFU/kg/day for 28 days. The current research shows that, *R. intestinalis* is a suitable next-generation probiotic considering its probiotic properties and safety.

KEYWORDS

probiotics, *Roseburia intestinalis*, safety, genome mining, oral toxicity, cytotoxicity, intestinal colonization

Introduction

Probiotics are defined as “live microorganisms that, when administered in adequate amounts, confer a health benefit on the host” (Salminen et al., 2021). The global market for probiotics is expected to reach \$91.1 billion by 2026, up significantly from \$61.1 billion in 2021.¹ Currently, most probiotic strains are derived from a limited number of bacterial species. These include *Lactobacillus* and *Bifidobacterium* species. Large-scale applications of metagenomic sequencing and bacterial genome editing methods have greatly expanded the range of bacteria with potential health benefits, and these bacteria are termed “Next Generation Probiotics” (NGPs; O’Toole et al., 2017). The development of NGPs requires preclinical research, safety testing, pharmacokinetics, pharmacodynamics, and Phase 1–3 clinical trials.

Roseburia intestinalis is an anaerobic bacterium that colonizes in the intestine and belongs to the phylum Firmicutes (Duncan et al., 2002; Nie et al., 2021). During colitis, *R. intestinalis* modulates the immune response and maintains tight junction integrity (Luo et al., 2019). Its flagellin regulates the long noncoding RNA HIF1A-AS2 (Quan et al., 2018), inhibits the activation of the NOD-, LRR- and pyrin domain-containing protein 3 (NLRP3) inflammasome (Wu et al., 2020), and stimulates the differentiation of regulatory T (Treg) cells to suppress colitis (Zhu et al., 2018). *R. intestinalis* inhibits intestinal inflammation by increasing the secretion of anti-inflammatory cytokines such as thymic stromal lymphopoietin (TSLP), transforming growth factor (TGF)- β , and interleukin (IL)-10 (Shen et al., 2018). Moreover, *R. intestinalis* alleviates colitis by affecting the brain-gut axis (Xu et al., 2021).

Roseburia intestinalis can also improve atherosclerosis (Kasahara et al., 2018; Liu et al., 2020) and alcohol-related liver diseases (Seo et al., 2020). There is evidence that the amount of *R. intestinalis* declines in patients with colorectal cancer (Montalban-Arques et al., 2021) and that treatment with the bacterium alone can prevent or even treat the disease (Liang et al., 2017). The abundance of *R. intestinalis* decreased in individuals suffering from amyotrophic lateral sclerosis (Nicholson et al., 2021), nonalcoholic steatohepatitis (Pan et al., 2021), pancreatic ductal adenocarcinoma (Zhou et al., 2021), and HIV infection (Dillon et al., 2017). *R. intestinalis* abundance was negatively correlated with waist circumference in patients with metabolic syndrome (Qin et al., 2021). Moreover, the bacterium has also been associated with graft-versus-host disease (Devaux et al., 2020) and insulin sensitivity in patients with type 2 diabetes (Lee et al., 2019). In fact, a recent study demonstrated *R. intestinalis* is associated with coronavirus disease 2019 (COVID-19), as the amount of the bacterium decreased significantly in severe patients (Xu et al., 2022). The relationship between *R. intestinalis* and various diseases is shown in Figure 1.

Currently, there are many guidelines related to probiotics, including those issued by the United States Food and Drug Administration (FDA), the World Gastroenterology Organization (WGO), the Product Safety Enforcement Forum of Europe (EU-PROSAFE; Vankerckhoven et al., 2008), and the International Scientific Association for Probiotics and Prebiotics (ISAPP; Hill et al., 2014). This study examined the safety and probiotic properties of *R. intestinalis* as well as its possible application in healthcare, in accordance with the above guidelines.

Materials and methods

Bacterial strains and culture conditions

Roseburia intestinalis L1-82 (DSMZ14610) was purchased from Deutsche Sammlung von Mikroorganismen und Zellkulturen GmbH (Braunschweig, Germany). *Bacteroides fragilis* (ATCC 25285) and *Bacteroides vulgatus* were obtained from Ningbo Mingzhou Biotechnology Co., Ltd. (Zhejiang, China). The above bacteria were cultured under anaerobic conditions at 37°C. An anaerobic culture environment was created using Atmosphere Generation Systems (AnaeroJar™ ASSEMBLY and AnaeroGen™, OXOID, Thermo Fisher Scientific). The culture medium (Miquel et al., 2015) was brain heart infusion (BHI) containing 0.5% yeast extract (OXOID), 1 mg/ml cellobiose (Macklin, China), 1 mg/ml maltose (Solarbio, China), 0.5 mg/ml cellobiose (Macklin, China), and 0.5 mg/ml cysteine (Solarbio, China). We established a standard curve to convert the absorbance values at 600 nm (OD600) to CFU values (Supplementary Figure S1). *Escherichia coli* ATCC 25922, *Staphylococcus aureus* ATCC 25923, *Salmonella typhimurium* CMCC 50115, *Bacillus subtilis* DSM 1088, and *Bacillus cereus* ATCC 11778 were used as controls. These strains were cultured in nutrient broth at 37°C in an aerobic environment.

Genotypic characterization

Screening the *Roseburia intestinalis* genome for safety and probiotic-related traits

Genome data for *R. intestinalis* were obtained from the National Center for Biotechnology Information (NCBI) database (GCF_900537995.1). The Comprehensive Antibiotic Resistance Database (CARD; Alcock et al., 2020) and Virulence Factor Database (VFDB; Liu et al., 2022) were used to predict virulence and antibiotic resistance genes. Genes related to biogenic amines, essential amino acids, and vitamin synthesis were identified in the bacterial genome using the Rapid Annotations using Subsystems Technology (RAST) server (Overbeek et al., 2014). The Carbohydrate-Active enZYmes (CAZy; Drula et al., 2021) database was used to analyze the carbohydrate metabolism ability of *R. intestinalis*.

¹ <https://www.marketsandmarkets.com/PressReleases/probiotics.asp>

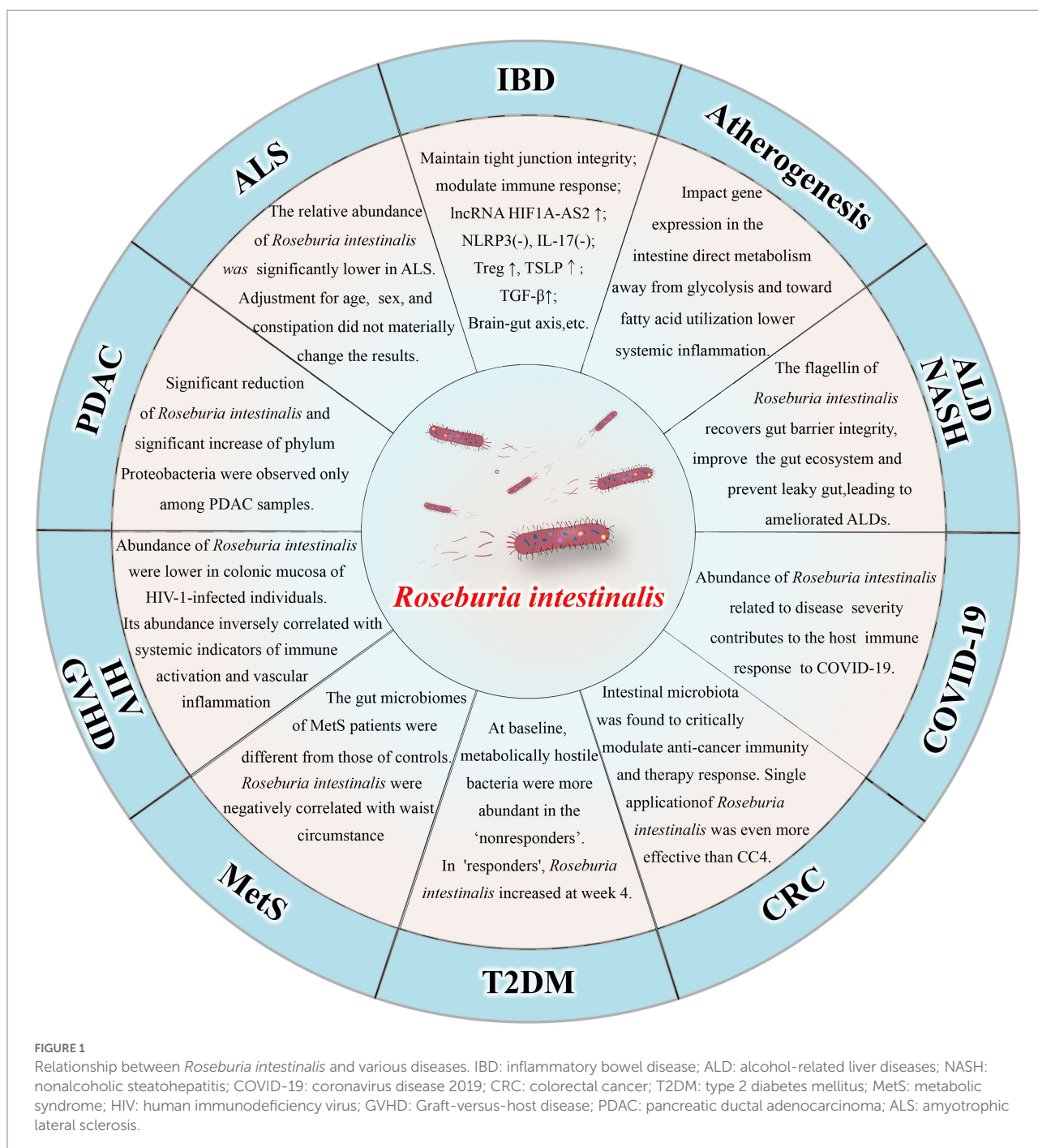
Prediction of the CRISPR-Cas system, prophages, bacteriocin, genomic islands, and primary metabolic gene clusters

CRISPRCasFinder was used to identify the CRISPR loci and associated Cas genes (Couvain et al., 2018). PHAge Search Tool Enhanced Release (PHASTER; Arndt et al., 2016) was used to identify and characterize the prophages within the genome. The bacteriocin operons were identified and visualized using BAGEL4 (van Heel et al., 2018). IslandViewer (Bertelli et al., 2017) was used to predict genomic islands (GIs) in the genome. All the above

predictions were made using default parameters. GutSMASH (Pascal Andreu et al., 2021) was used to identify and analyze specific gene clusters associated with primary metabolism and energy capture.

Comparative genomic analysis

Several bacterial strains considered potential probiotics or pathogens in inflammatory bowel disease (IBD) were selected, and their genomes were compared with that of *R. intestinalis*. This included strains of *R. intestinalis* and other species of the genus *Roseburia*. GenBank accession numbers for these strains are listed in



Supplementary Table S1. Genes involved in acid or bile salt tolerance, intestinal adhesion colonization, and antioxidant activity were retrieved from a previous study (Hussein et al., 2020) and aligned using the NCBI Basic Local Alignment Search Tool (BLAST) tools. We aligned the query genome with that of *R. intestinalis* using the BLAST Ring Image Generator (BRIG; Alikhan et al., 2011).

Phenotypic safety assessment of probiotic characteristics

Acid tolerance

Acid tolerance was tested as previously described (Anandharaj et al., 2015). The bacterium was grown anaerobically at 37°C for 24 h, centrifuged at 4000 rpm for 10 min, and the suspension was washed twice with phosphate-buffered saline (PBS). We used 1 M HCl to adjust the pH of the medium in order to simulate the acidic environment of the stomach. *R. intestinalis* was added to the medium at varying pH values and cultured at 37°C for 24 h. Viable cells were counted on BHI agar plates, and the results were expressed as log₁₀ colony-forming units (CFU)/ml.

Cell surface hydrophobicity

CSH was measured as described previously (Sharma et al., 2019). *R. intestinalis* in logarithmic growth phase was washed twice and resuspended in PBS, with the density adjusted to between 0.8 and 1.0. The n-hexadecane and bacterial solution were mixed at a ratio of 1:5 (v:v), and the mixture was vortexed for 2 min. The mixture was kept at room temperature for 45 min, and the aqueous phase was used to determine the OD600. CSH was calculated using the following formula:

$$\text{CSH} (\%) = \frac{A_0 - A}{A_0} \times 100.$$

A₀ and A represent the OD600 values measured before and after mixing with n-hexadecane, respectively.

Auto-aggregation and co-aggregation

Auto-aggregation ability was identified based on the method described by Reuben et al. (2020), with slight modifications. The bacterium was rinsed twice and resuspended in PBS, and the OD600 was adjusted to 1.0 (A₀). The bacterial suspension was incubated at 37°C for 2–24 h, and the OD600 of the supernatant was measured. Auto-aggregation capacity was calculated using to the following formula:

$$\text{Auto-aggregation} (\%) = \left(1 - \frac{A_t}{A_0}\right) \times 100.$$

Co-aggregation ability was examined using a previously described method (Soleri et al., 2014). Equal volumes of *R. intestinalis* and pathogenic bacterial suspensions were mixed and vortexed for 10 s. A suspension of each bacterium alone was used as a control. A series of OD600 measurements were taken

at different time points. The co-aggregation was calculated as follows:

$$\text{Co-aggregation} (\%) = [1 - \frac{A(x+y)}{(Ax+Ay)/2}] \times 100.$$

For each time point, Ax represents the OD600 of *R. intestinalis*, and Ay represents the absorbance of each pathogenic bacterium.

Bile salt tolerance

The bile salt tolerance test was performed as previously described (Hussein et al., 2020). *R. intestinalis* at 10⁸ CFU/ml was inoculated into BHI medium containing 0.3% porcine bile salts (Solarbio, China). To simulate human intestinal conditions, 200 µl of bacterial broth was seeded in a 96-well microplate and incubated in an anaerobic incubator at 37°C for 0–8 h. Bacterial growth was monitored hourly by measuring OD600.

Bacterial adhesion to epithelial intestinal cells

The ability to adhere to intestinal epithelial cells was evaluated in a manner similar to that reported by Dudík et al. (2020). Caco-2 and HT-29 cells were cultured in Roswell Park Memorial Institute (RPMI)-1,640 medium containing 10% fetal bovine serum (Procell, China), seeded in six-well plates, and the medium was changed every 48 h. The cells were cultured continuously for 21 days. Bacteria were washed and resuspended in PBS (OD600 = 1.0). The plate was placed in a cell incubator at 37°C for 1 h with 1 ml of bacterial solution added to each well. The plate was rinsed three times with PBS, and 1 ml of 0.05% trypsin was added to digest the cells. The digested cell suspension was serially diluted in PBS and colonies were counted on BHI agar plates.

Hemolysin activity

The hemolytic activity experiments were based on Sonakshi et al. (Rastogi et al., 2020). *R. intestinalis* was inoculated onto BHI agar containing 5% (v/v) sterile defibrillated sheep blood, and cultured at 37°C under anaerobic conditions for 72 h. A clear halo around the colony indicates β-hemolysis, a green halo indicates α-hemolysis, and no halo indicates γ-hemolysis. *S. aureus* ATCC 25923 was used as a positive control.

DNase activity

DNase activity was measured using a previously described method (Rastogi et al., 2020). *R. intestinalis* was inoculated onto DNase agar medium (Hopebio, China) for 72 h. A solution of 1 M HCl was then added to the plate and the colonies were observed after a few minutes to determine whether a clear area was present around them. The positive control bacteria were *S. aureus* ATCC 25923 and the negative control bacteria were *E. coli* ATCC 25922.

Gelatinase activity

Approximately 50 µl of bacterial suspension (10⁹ CFU/ml) was added to a gelatin biochemical detection tube (Hopebio, China) and incubated at 37°C for 48 h. The tube was placed in a

refrigerator for 20 min, and tilted to observe whether the medium could solidify. If the medium is liquid, gelatin is hydrolyzed and gelatinase activity is positive. *Bacillus cereus* ATCC 11778 was used as a positive control and *E. coli* ATCC 25922 was used as a negative control.

Detection of biofilm formation

Roseburia intestinalis was resuspended in the BHI medium and adjusted to a concentration of 10^7 CFU/ml. Next, 200 μ l of the bacterial suspension was added to a 96-well plate, and the plate was incubated at 37°C for 72 h in an anaerobic jar. The wells were rinsed thrice with PBS. Then, 200 μ l of methanol was added to each well, and the methanol was removed after fixing for 15 min. Subsequently, 200 μ l of 1% crystal violet was added, and the wells were washed three times with PBS after 15 min. After air-drying for 30 min, 200 μ l of 30% glacial acetic acid was added to the plate. The liquid in the well was transferred to a new plate and the OD₅₅₀ was measured. A 30% glacial acetic acid solution was used as blank control. As controls, we selected two anaerobic (*Bacteroides fragilis* and *Bacteroides vulgatus*) and one aerobic probiotic (*B. subtilis*), in addition to three other pathogens (*E. coli*, *S. aureus*, *S. typhimurium*). Using the average OD (ODc) of the negative control group as a cut-off value, the bacteria were categorized into those without biofilm (OD ≤ ODc), weak (ODc < OD ≤ 2ODc), moderate (2 ODc < OD ≤ 4ODc) and strong (OD > 4ODc) biofilm formation (Cozzolino et al., 2020).

Antibiotic susceptibility

According to European Food Safety Authority, probiotics must be tested for resistance to the following 9 antibiotics: ampicillin, vancomycin, gentamicin, kanamycin, streptomycin, erythromycin, clindamycin, tetracycline, and chloramphenicol. The disk diffusion method (Rocha-Mendoza et al., 2020) was used to determine the susceptibility of *R. intestinalis* to 17 antibiotics. By measuring the zone of inhibition according to Clinical and Laboratory Standards Institute (CLSI) criteria (CLSI, 2016), we were able to determine the susceptibility of the bacteria to antibiotics.

Inhibition of pathogen internalization

Three different methods (Fan et al., 2019) were used to examine the ability of *R. intestinalis* to defend against pathogen invasion of epithelial cells. HT-29 cells infected with 1×10^7 CFU/ml of *E. coli* (multiplicity of infection [MOI] = 100) and incubated for 2 h served as a control group.

For the competition test, 1×10^8 CFU/ml of *R. intestinalis* and 1×10^7 CFU/ml of *E. coli* were added simultaneously to the cells and incubated for 2 h. For the displacement test, cells were first incubated with 1×10^7 CFU/ml of *E. coli* for 1 h, and then 1×10^8 CFU/ml of *R. intestinalis* was added and incubated for 1 h. For the exclusion test, HT-29 cells were first pre-incubated with 1×10^8 CFU/ml of *R. intestinalis* for 1 h, followed by the addition of 1×10^7 CFU/ml of *E. coli* for 1 h at 37°C. All groups were washed with PBS and the medium was changed to

RPMI-1640 containing 1% penicillin/streptomycin/gentamicin (Biosharp, China) and incubated for 2 h at 37°C. To count intracellular *E. coli*, the cells were dissociated with 0.05% trypsin and treated with 0.1% Triton X-100 for 8 min. Results are expressed as the percentage decrease in *E. coli* invasion into cells in the experimental group compared with the control group.

Determination of cytotoxicity

Cell culture

Two human colorectal cancer cell lines, HT-29 and Caco-2, as well as the normal human colon epithelial cell line NCM460, were cultured at 37°C in a humidified environment containing 5% CO₂ in RPMI-1640 medium containing 10% fetal bovine serum (Procell, China). After the cells had grown to 80–90% confluence, they were digested with 0.05% trypsin and seeded into appropriate cell culture plates according to the experimental procedure.

Cell viability assay

The effect of *R. intestinalis* on cell viability was evaluated using a cell counting kit (CCK-8 assay). *R. intestinalis* was co-cultured with the cells for 4 h at an MOI of 100. The bacteria-containing medium was replaced with medium supplemented with 1% penicillin/streptomycin/gentamicin, followed by incubation at 37°C for 2 h to eliminate all extracellular bacteria (Li et al., 2021). For further experiments, the medium was changed to normal RPMI-1640 medium and cell viability was evaluated at different time points. The control group consisted of cells treated with *E. coli*.

Activity of lactate dehydrogenase

Roseburia intestinalis (10^8 CFU/ml) was co-cultured with the NCM460 cells at 37°C for 4 h. Lactate dehydrogenase (LDH) released by the damaged cells was measured using an LDH assay kit (Beyotime, China). The results were expressed as a percentage of LDH activity in each group relative to the positive control reagent provided by the kit (Hussein et al., 2020).

Calcein-propidium iodide staining in live and dead cell detection test

HT-29 cells were co-cultured with bacteria (10^8 CFU/ml) for 4 h, followed by a change to media containing 1% penicillin/streptomycin/gentamicin, and cultured for two additional hours at 37°C. The tests were conducted according to the manufacturer's instructions (Beyotime, China), and the relative fluorescence values (RFU) were compared between the experimental and control groups.

Edu cell proliferation test

HT-29 cells were cultured in 6-well plates. As soon as the cells reached 80% confluence, 100 μ l of *R. intestinalis* or *E. coli* (10^8 CFU/ml) was added to the plate, and 30 μ M of DNA synthesis

inhibitor (hydroxyurea, Beyotime) served as the positive control. An EdU Cell Proliferation Kit (Beyotime) was used to detect cell proliferation after 24 h. The FUJI-ImageJ software was used to quantify the percentage of EdU-positive cells (Lu et al., 2019).

Spatial and temporal distribution of *Roseburia intestinalis* within the gastrointestinal tract

Carboxyfluorescein diacetate succinimidyl ester staining of *Roseburia intestinalis*

The bacteria were centrifuged at 12000 rpm for 5 min and washed thrice with PBS. An equal volume of 1× CFDA-SE staining solution (Beyotime) was added to the bacterial suspension, and the mixture was incubated for 30 min at 37°C in the dark. The samples were then washed thrice with PBS to remove the unbound dye. Fluorescence was observed using a fluorescence microscope at an excitation wavelength of 488 nm.

Intestinal distribution of *Roseburia intestinalis* in C57BL/6J mice

To investigate the characteristics of *R. intestinalis* colonization of the GIT, we used a previously described method (Zhao et al., 2022). *R. intestinalis* was collected during the logarithmic growth phase, stained with CFDA-SE, and resuspended in PBS at a concentration of 1×10^{10} CFU/ml. The mice were then gavaged with 200 µl of bacterial solution, whereas the control group was administered PBS. Mice were euthanized 2 to 72 h after gavage, and 1 cm long sections of the duodenum, jejunum, ileum, cecum, colon, and rectum were removed. After thoroughly rinsing the intestinal tube with PBS, the particulate matter was filtered using a 40 µm cell strainer. Flow cytometry (Cytek Athena™) was used to analyze the ratio of CFDA-SE labelled *R. intestinalis* in the intestine. Mice gavaged with non-fluorescently labelled *R. intestinalis* were used as blank controls.

For frozen sections, mice were euthanized 12 h after administration of *R. intestinalis*, cecal and colonic specimens were collected and washed in sterile PBS, embedded with Optimal cutting temperature (OCT) reagent (Sakura, Japan), and frozen sections were obtained immediately (Leica CM1950).

Cecal microbiota

To analyze the effect of *R. intestinalis* on the structure of the intestinal flora, mice were gavaged with *R. intestinalis* at a concentration of 1×10^9 CFU/ml for 14 days. On days 7 and 14, mouse feces were harvested for 16S rRNA sequencing.

A MagPure Stool DNA kit (Magen, China) was used to extract DNA from the microbial communities. DNA was quantified using a Qubit Fluorometer with the Qubit dsDNA Kit (Invitrogen, United States), and quality was checked using a 1% agarose gel. Polymerase chain reaction (PCR) primers 341F (5'-ACTCCTACGGGAGGCAGCAG-3') and 806R (5'-GGACTACHVGGGTWTCTAAT-3') were used to amplify

the variable regions V3–V4 of the bacterial 16S rRNA genes. The primers were tagged with Illumina adapter, pad, and linker sequences. PCR enrichment was performed using a 50 µl reaction containing 30 ng template, fusion PCR primer, and master mix. The PCR cycling conditions were 94°C for 3 min, 30 cycles of 94°C for 30 s, 56°C for 45 s, 72°C for 45 s, and 10 min at 72°C for extension. PCR products were purified using AmpureXP beads and eluted with elution buffer. The libraries were qualified using an Agilent 2,100 bioanalyzer (Agilent, United States). The validated libraries were sequenced on an Illumina MiSeq platform (BGI, Shenzhen, China) following the standard Illumina pipeline and 2 × 300 bp paired-end reads were generated.

In vivo toxicology studies

Animals and tests organisms

Oral toxicity studies were performed using male C57BL/6J mice (6–8 weeks) and all animal experiments were approved by the Central South University Animal Ethics Committee (XMSB-2022-0198). The animals were housed under standard conditions with alternating periods of light and dark (12 h each) at a temperature of $25 \pm 2^\circ\text{C}$ and with free access to food and water. The animals were acclimated for 7 days before the experiment. *R. intestinalis* was cultured in an anaerobic environment at 37°C for 24 h in the BHI medium. Bacteria were centrifuged for 10 min at 4000 rpm, rinsed, and resuspended in PBS.

Acute oral toxicity study

The acute oral toxicity test was conducted according to the method described by Anantha et al. (Metlakunta and Soman, 2020) and the Organisation for Economic Co-operation and Development (OECD) guideline No.423 with certain modifications. This study was conducted in a stepwise manner. As a first step, three mice (group A1) were gavaged with *R. intestinalis* at a dose of 1.9×10^9 CFU/kg. It represents 133–1,330 times the empirical dose level of oral probiotics in humans (i.e., $108\text{--}10^9$ CFU or $1.43 \times 10^6\text{--}1.43 \times 10^7$ CFU/kg day in a 70 kg individual; Steppe et al., 2014). In the following 48 h, there were no mortality, morbidity, or abnormal clinical signs. To confirm this, the same dosage was administered to another group (A2), while a control group of mice (A0) was administered PBS. The animals were monitored for 14 consecutive days for clinical manifestations, such as changes in the skin and fur, mucous membranes, respiration, and behavioral changes. The animals were euthanized at the end of the observation period, and the gross appearance of vital organs, organ weights, and histopathology were assessed. Blood was collected from the animals for biochemical and hematological analyses.

28-day repeated dose toxicity study

According to OECD No.407, this part of the study evaluated the toxicity of *R. intestinalis* after repeated administration for 28 days to establish dose-response

relationships and determine the NOAEL. Each group consisted of six mice, and the control group (S0) was administered PBS *via* gavage. The experimental groups were divided into three dose levels corresponding to 66–657 times (S1), 77–769 times (S2), and 92–923 times (S3) the empirical dose of oral probiotics in humans. The mice were monitored daily for changes in clinical signs, mortality, fur and skin, respiration, behavioral patterns, body weight, food intake, and water consumption. On the 29th day, the mice were euthanized and blood samples were collected for analysis of hematology and biochemical indicators. The gross appearance of vital organs, organ weights, and histopathology were assessed.

Statistical analysis

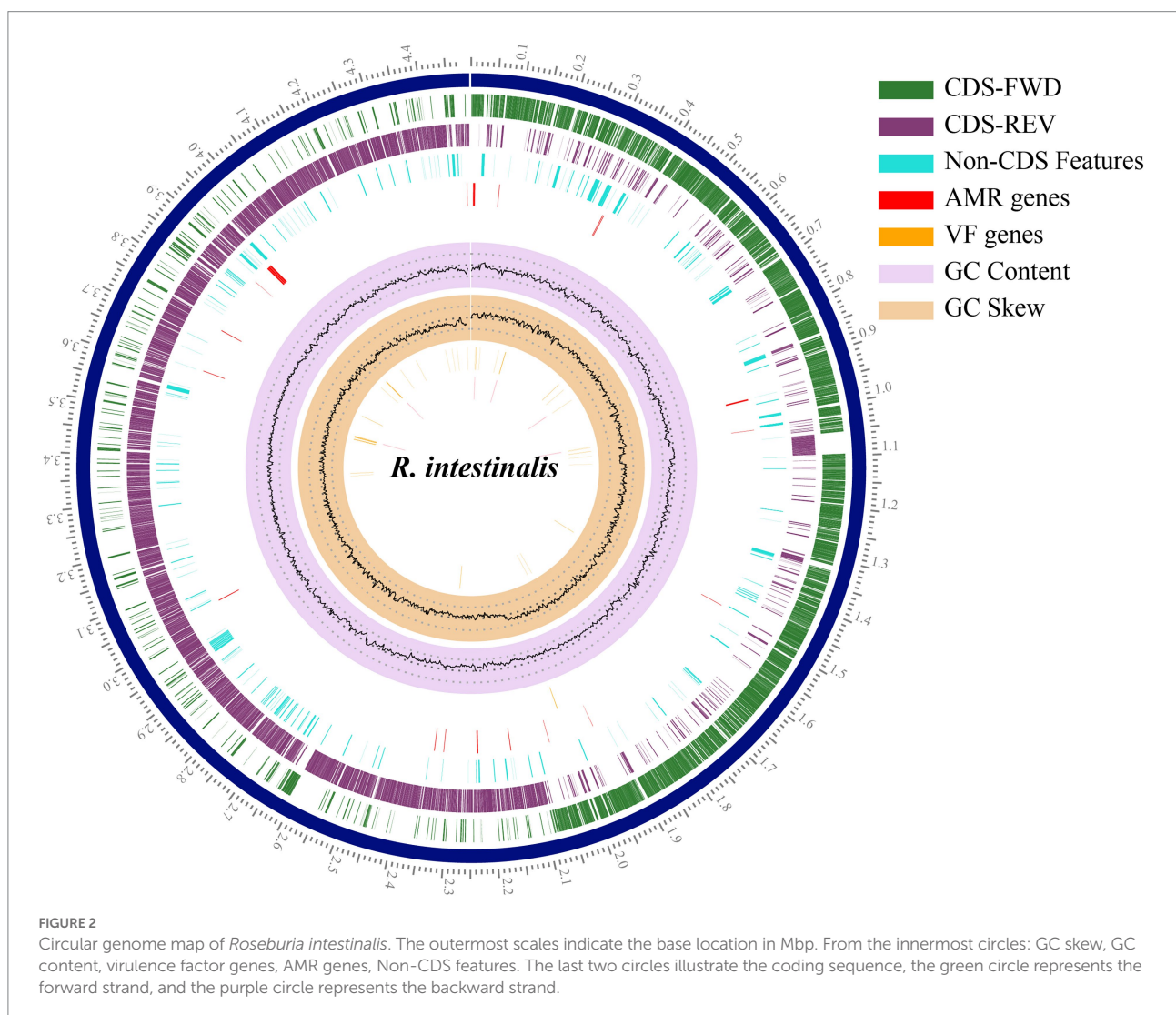
Statistical analyses were performed using SPSS version 25.0. To ensure homogeneity of variance and normality of the data, the Kolmogorov–Smirnov test was used. The values are presented as the mean \pm standard deviation for normally distributed data or as

the median and interquartile range for data that were not normally distributed. When comparing two groups, *p* values were derived from the Student's t-test for normally distributed data, and the Mann–Whitney was used for data with other distributions. For multi-group comparisons, *p* values were determined using one-way ANOVA. We considered *p* < 0.05 statistically significant in all comparisons.

Results

Genome annotation

The RAST annotation results indicated that the genome contained 4,340 coding sequences and 81 RNA genes ([Supplementary Figure S2](#)). In total 252 subsystems were functionally annotated. Carbohydrates accounted for the largest number of genes (200), followed by amino acids and derivatives (192). Pathosystems Resource Integration Center (PATRIC; [Davis et al., 2020](#)) was used to generate a circular genome map ([Figure 2](#)).



Safety and probiotic-related traits in *Roseburia intestinalis* genome

In *Roseburia intestinalis*, we detected three CRISPR sequences and two Cas genes. The CRISPR sequences were located at 1020388–1020441 bp, 1,222,931–1,223,608 bp, and 1,225,355–1,226,103 bp, while the Cas gene sites were located at 1015665–1019051 bp and 1,216,581–1,217,327 bp. The genome contained no genes involved in biogenic amine biosynthesis other than spermidine synthase (*speE*) and carboxynorspermidine decarboxylase (*nspC*). The genome contains essential amino acid synthesis genes (tryptophan, methionine, threonine, arginine, and cysteine), as well as vitamin synthesis genes (i.e., Thiamine, Riboflavin, Folate, Pantothenate, and Biotin; **Table 1**).

Prophages, bacteriocins, metabolic gene clusters, carbohydrate-active enzymes, and genomic islands

PHASTER identified seven prophages within the genome, of which three are incomplete and four are questionable. The details of the prophages are provided in **Supplementary Table S2**. Using the BAGEL4 webserver, we detected that the bacterium harbored a bacteriocin cluster (**Figure 3C**) of Zoocin A class within contig 93.3 (3723994–3,744,393 bp). AOI consisted of

RNA pseudouridine synthase, a transcriptional regulatory protein (LanR), a putative lantibiotic resistance two-component sensor kinase precursor (LanK), and multiple open reading frames (ORFs). Using gutSMASH, we discovered that the genome contained six metabolism-related gene clusters (**Table 2**). Four of these clusters are associated with short-chain fatty acid metabolism, including butyric acid synthesis.

The CAZy database identified 222 carbohydrate-active enzyme modules in the genome. A total of 136 glycoside hydrolase families, 48 glycosyltransferases, 14 carbohydrate esterase families, and 24 carbohydrate-binding module families were identified. Using IslandViewer, we combined two prediction algorithms, islandPath-DIMOB and SIGI-HMM, and identified 41 GIs (**Supplementary Figure S3**). In the predicted GIs, no annotated virulence, antibiotic resistance, or pathogenicity genes were identified.

Comparative genomic analysis

The genome contains *tetO* and *Tet(40)*, which are associated with tetracycline resistance, whereas other *Roseburia* genera and other probiotic/pathogenic bacteria contain more antibiotic resistance genes (**Figure 3A**). According to VFDB, the *R. intestinalis* genome contains genes related to adhesion (*fbpA/fbp68, ebpC, efaA, plr/gapA*), and lipid and fatty acid metabolism (*pand*; **Figure 3B**). Compared to other probiotics (all belonging

TABLE 1 Associated biosynthetic genes detected in *R. intestinalis* genome about essential amino acids or vitamins.

Category	Name	KO	Gene	Biosynthesis protein
Essential amino acid	Tryptophan	ko: K01695	trpA	tryptophan synthase alpha chain
		ko: K01696	trpB	tryptophan synthase beta chain
		ko: K01867	WARS	tryptophanyl-tRNA synthetase
		ko: K00789	metK	S-adenosylmethionine synthetase
		ko: K02071	metN	D-methionine transport system ATP-binding protein
		ko: K02072	metL	D-methionine transport system permease protein
		ko: K02073	metQ	D-methionine transport system substrate-binding protein
		ko: K01733	thrC	threonine synthase
		ko: K01620	ltaE	threonine aldolase
		ko: K04720	cobD	threonine-phosphate decarboxylase
	Arginine	ko: K01585	speA	arginine decarboxylase
Vitamins	Cysteine	ko: K01738	cysK	cysteine synthase
		ko: K04487	iscS	cysteine desulfurase
	Thiamine	ko: K00788	thiE	thiamine-phosphate pyrophosphorylase
		ko: K00949	thiN	thiamine pyrophosphokinase
	Riboflavin	ko: K00793	ribE	riboflavin synthase
		ko: K11754	folC	dihydrofolate synthase / folylpolyglutamate synthase
	Folate	ko: K00287	DHFR	dihydrofolate reductase
	Pantothenate	ko: K03525	coaX	type III pantothenate kinase
		ko: K01012	bioB	biotin synthase

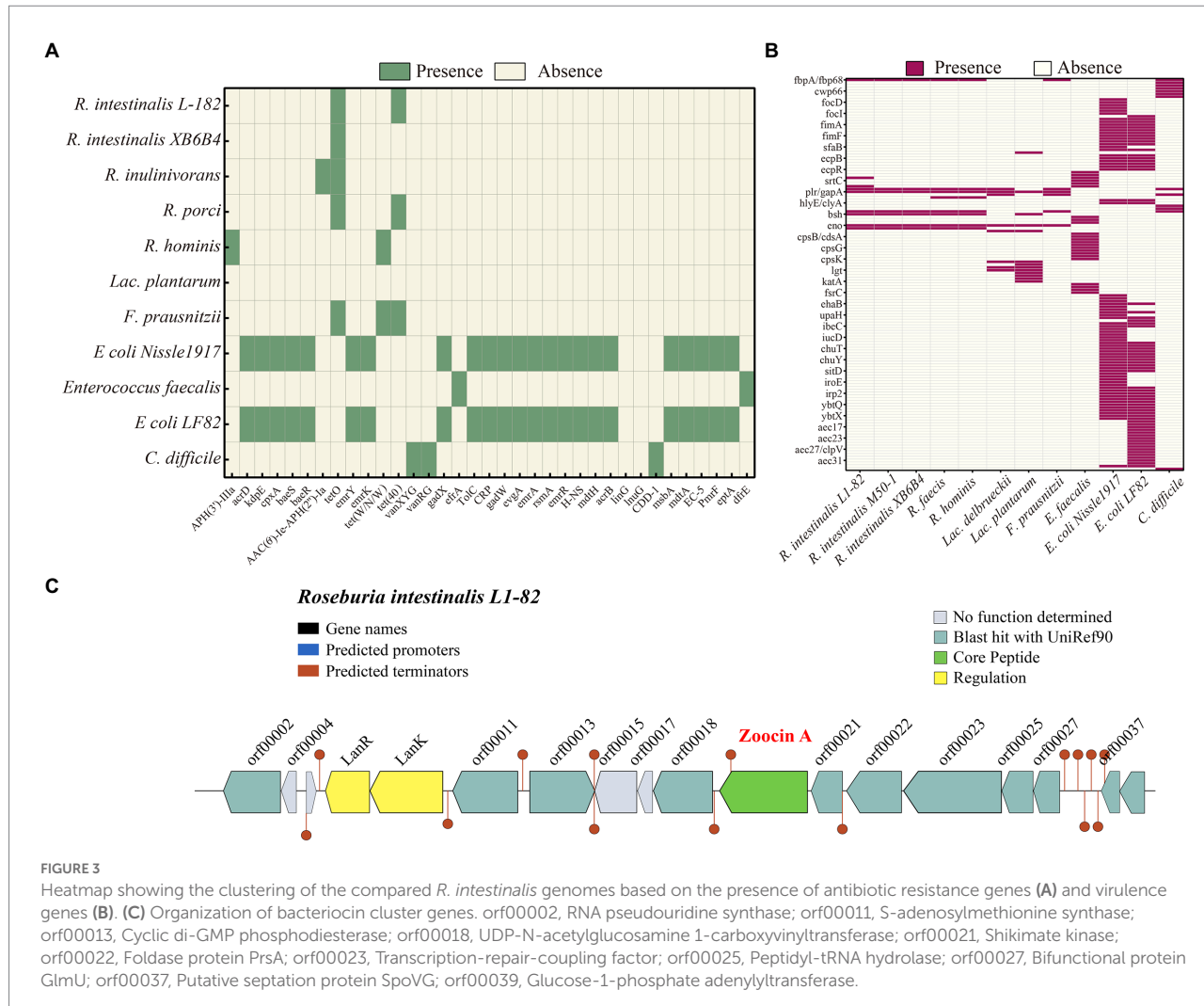


FIGURE 3

Heatmap showing the clustering of the compared *R. intestinalis* genomes based on the presence of antibiotic resistance genes (A) and virulence genes (B). (C) Organization of bacteriocin cluster genes. orf00002, RNA pseudouridine synthase; orf00011, S-adenosylmethionine synthase; orf00013, Cyclic di-GMP phosphodiesterase; orf00018, UDP-N-acetylglucosamine 1-carboxyvinyltransferase; orf00021, Shikimate kinase; orf00022, Foldase protein PrsA; orf00023, Transcription-repair-coupling factor; orf00025, Peptidyl-tRNA hydrolase; orf00027, Bifunctional protein GlmU; orf00037, Putative septation protein SpoVG; orf00039, Glucose-1-phosphate adenyltransferase.

TABLE 2 Identified primary metabolite regions by gutSMASH.

Region	Type	Class	From	To	Core biosynthetic genes	Similarity
1	porA	SCFA	54,788	78,257	porB,porC	
2	acetate to butyrate	SCFA	642,855	668,098	thlA, hbd,bcd, carD,carE	83%
3	Rnf complex,succinate to propionate	SCFA	2,259,537	2,304,034	mcp1,rsxB2,rsxA, rnfE,rsxG,rsxD, rsxC,gcdB,pccB	100%
4	Putrescine to spermidine	Aliphatic amine	3,070,869	3,094,310	nspC,speE	100%
5	Others HGD unassigned	Putative	3,145,614	3,169,501	hgdC	
6	Pyruvate to acetate-formate	SCFA	3,615,206	3,638,200	pflA,pflB	100%

to Firmicutes), *R. intestinalis* contains more genes that encode cell adhesion-related proteins and genes related to gastrointestinal survival (Supplementary Figure S4). The genome contains seven genes related to antioxidant activity, suggesting a strong ability to survive in the host environment. Furthermore, we compared its genome with the genomes of six probiotics and found that *F. prausnitzii*, a probiotic used in the treatment of IBD (Machiels et al., 2014), possessed the highest degree of similarity (Supplementary Figure S5).

Phenotypic safety assessment of probiotic characteristics

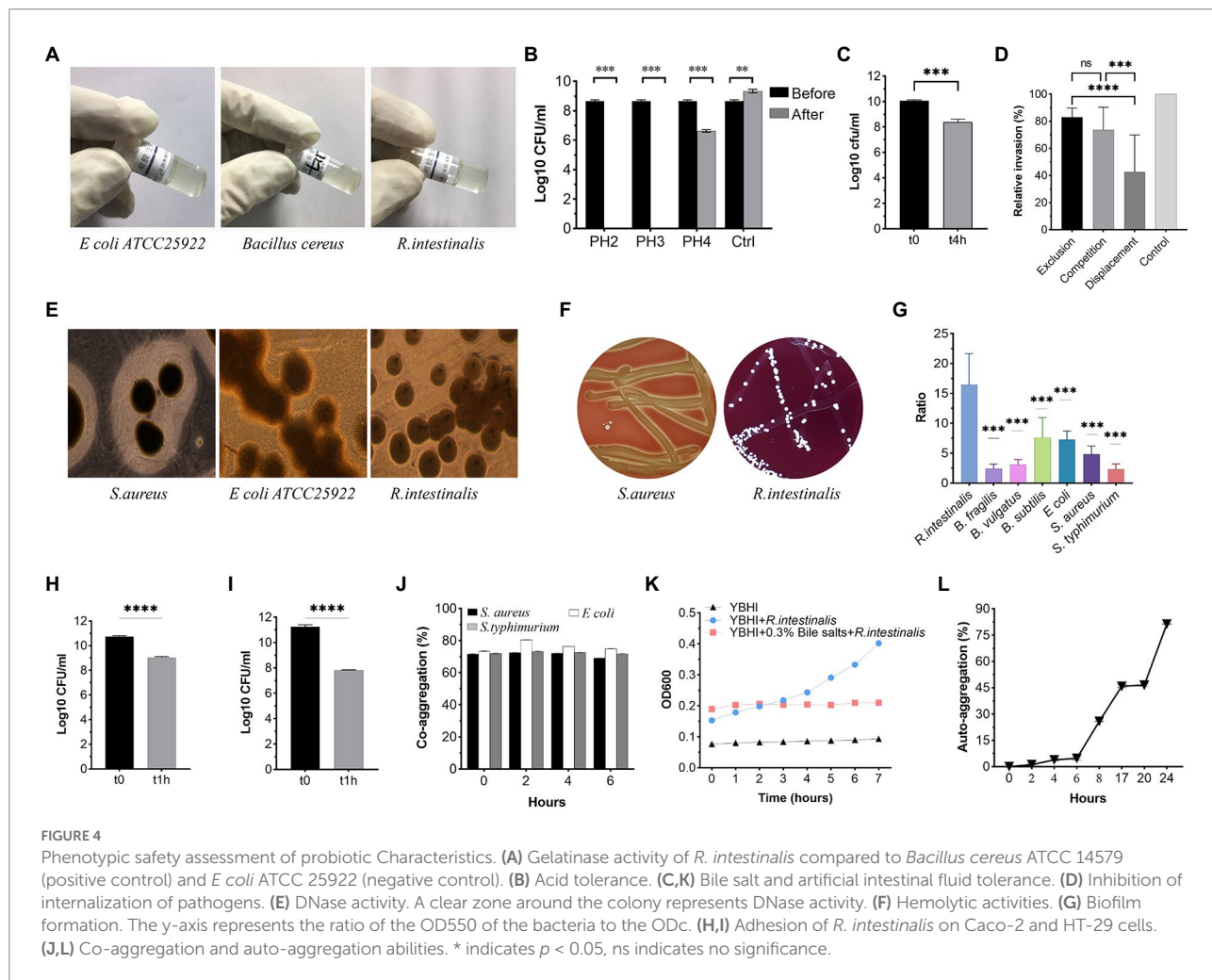
R. intestinalis was tested for its resistance to 17 antibiotics (Table 3). The bacterium was sensitive to most antibiotics, had intermediate resistance to streptomycin and kanamycin, and was only resistant to amikacin.

As shown in Figure 4, *R. intestinalis* exhibited no gelatinase, (Figure 4A) DNase (Figure 4E), or hemolytic activity. As a

TABLE 3 Antibiotic susceptibility of selected antibiotics tested against *R. intestinalis*.

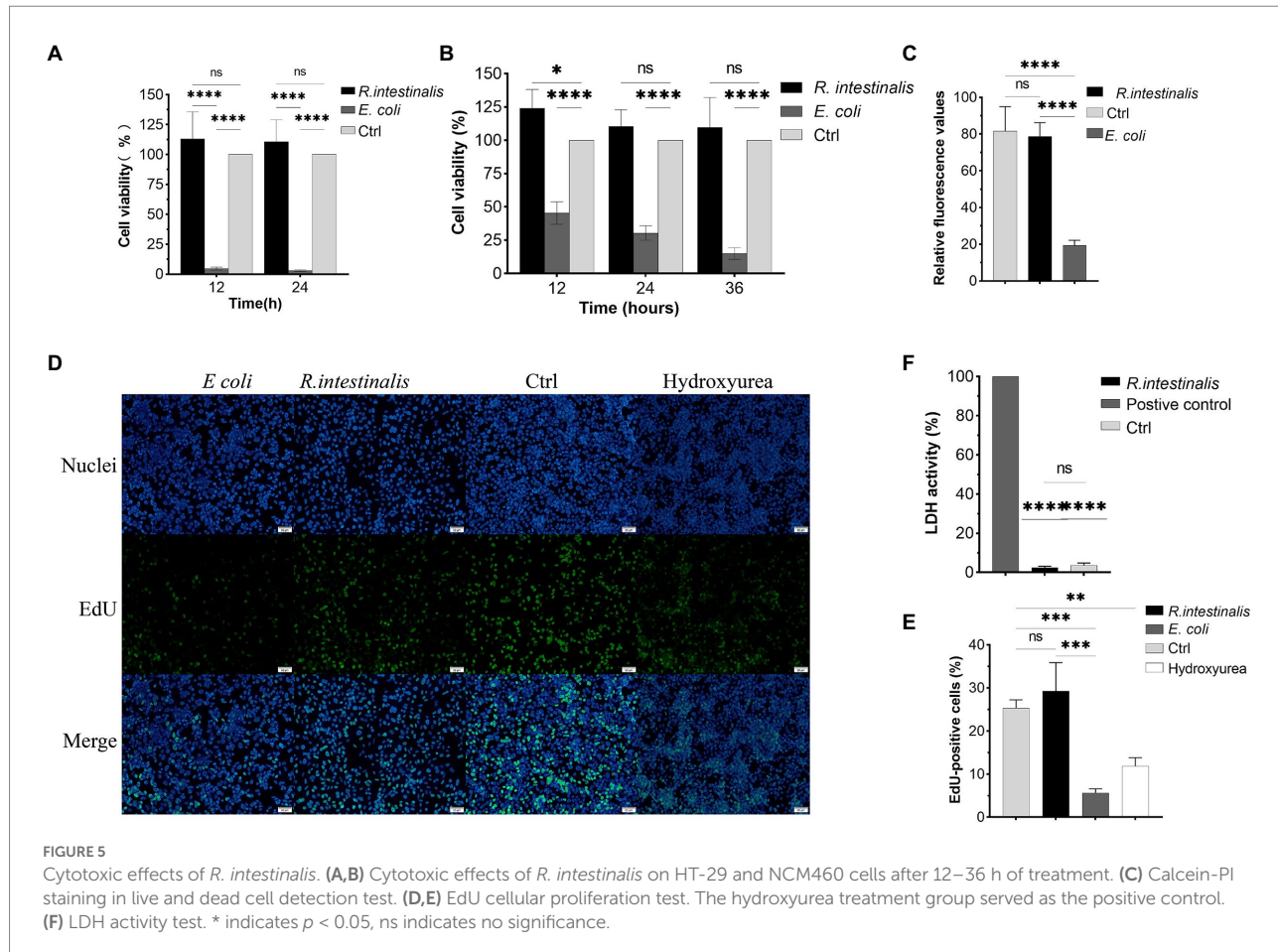
Antibiotic	ZOI (mm)	Antibiotic susceptibility	Antibiotic	ZOI (mm)	Antibiotic susceptibility
Amikacin	13.5 ± 0.41	R	Penicillin	46.1 ± 0.25	S
Ampicillin	19.6 ± 0.46	S	Gentamicin	17.6 ± 0.49	S
Erythromycin	48.4 ± 0.29	S	Tetracycline	27.7 ± 0.53	S
Kanamycin	14.1 ± 0.22	I	Cefuroxime	36.7 ± 2.05	S
Clindamycin	40.2 ± 0.54	S	Cefoperazone	39.7 ± 4.49	S
Chloramphenicol	38.9 ± 1.63	S	Ceftriaxone	40.7 ± 3.09	S
Streptomycin	14.5 ± 0.45	I	Ceftazidime	21.3 ± 0.47	S
Minocycline	40.7 ± 1.69	S	Vancomycin	27.5 ± 0.33	S
Piperacillin	37.8 ± 0.85	S			

S: susceptible; I: intermediate; R: resistant; ZOI: Zone of growth inhibition.



positive control, *S. aureus* ATCC 25923 exhibited β -hemolysis (Figure 4F). *R. intestinalis* survived in an environment with a pH of 4 (Figure 4B). The proliferation of bacteria was inhibited in the presence of 0.3% bile salt, whereas bacteria survived in the artificial intestinal fluid (Figures 4C,K). *R. intestinalis* was able to adhere effectively to HT-29 and Caco-2 cells (Figures 4H,I) and

exhibited a hydrophobicity of $12.25 \pm 1.01\%$ in n-hexadecane. At 24 h, *R. intestinalis* had a maximum auto-aggregation ability of 80% (Figure 4L), and the co-aggregation experiment (Figure 4J) showed a strong co-aggregation ability (69–80%). Competition, displacement, and exclusion experiments showed that *R. intestinalis* inhibited the internalization of *E. coli* into epithelial



cells (Figure 4D). *R. intestinalis* had a higher biofilm-forming ability than several probiotics and pathogens (Figure 4G). This may allow it to gain a competitive growth advantage and enhance its ability to adhere to the intestinal epithelium.

Cytotoxicity

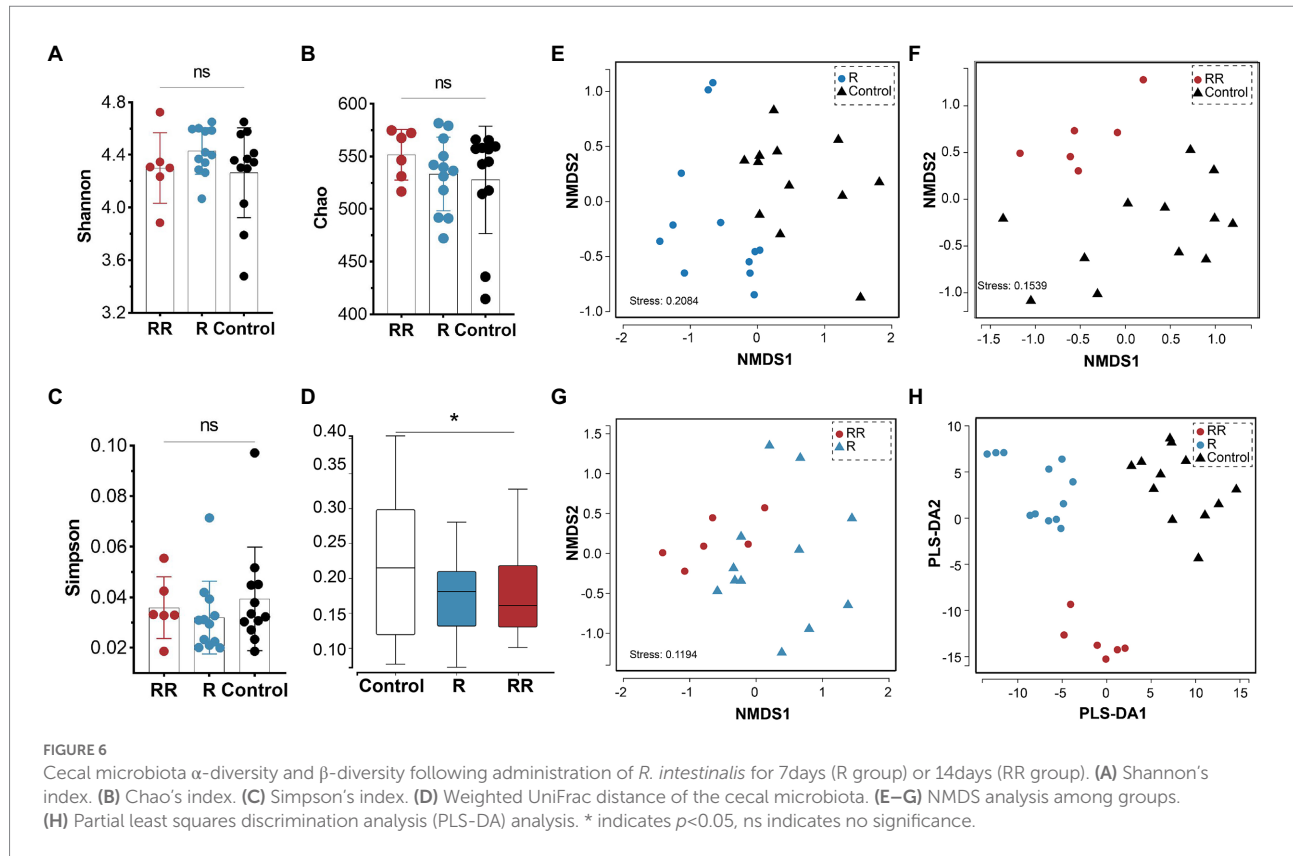
After treatment with *R. intestinalis*, there was no statistically significant difference in cell viability between the experimental and control groups ($p > 0.05$); however, cell viability was significantly reduced after treatment with *E. coli* (Figures 5A,B). As shown in Figure 5C, the RFU of the experimental group was not significantly different from that of the control group, whereas that of the *E. coli* treatment group was significantly different ($p < 0.05$). Compared to the positive control, there was no significant difference in LDH activity between the *R. intestinalis* treatment and control groups. This indicates that this probiotic bacterium did not cause notable cell damage (Figure 5F). The proportion of EdU-positive cells in the treatment group did not differ significantly from that in the control group but differed significantly from that in the positive control group ($p < 0.05$). This indicated that *R. intestinalis* treatment did not affect DNA replication during cellular proliferation (Figures 5D,E).

Cecal microbiota

There was no statistically significant difference among the groups in any of the α -diversity indices (Figures 6A–C), indicating that oral administration of *R. intestinalis* did not modify gut microbiota diversity and abundance. Non-metric multidimensional scaling (NMDS) analysis using a weighted UniFrac analysis revealed distinct differences in microbiota structure (Figures 6D–H). We found that the highest relative abundance of *R. intestinalis* occurred 7 days after oral administration (Figures 7A–C). Species with core effects were analyzed using the LEfSe method. The core strains after 7 days of administration were *Firmicutes*, *Clostridiales*, *Clostridia*, *Lachnospiraceae* among others. After 14 days, the core species were *Barnesiella* and *Porphyromonadaceae* (Figure 7D). The PICRUSt tool based on the Kyoto Encyclopedia of Genes and Genomes (KEGG) database was used to predict pathway enrichment, and we observed differences in pathway enrichment after the administration of *R. intestinalis* (Supplementary Figure S6).

Colonization characteristics of *Roseburia intestinalis* using fluorescent labelling

Two hours after oral administration, fluorescently labelled bacteria (Figure 8A) were detected in all intestinal segments, with



the highest concentration in the colon. After 48 h, the content of *R. intestinalis* in the cecum exceeded that in the colon. After 72 h, the bacterium primarily colonized the cecum and colon, whereas its distribution in the duodenum, jejunum, ileum, and rectum was scarce (Figure 8B; Supplementary Figure S7). The results of the frozen section demonstrated that the spatial colonization sites of *R. intestinalis* were primarily located in the cecum and colonic mucus layers (Figure 8C).

Acute toxicity study

During observation period, no mortality, morbidity, or abnormal clinical manifestations were observed. The average daily food and water intake is presented in Supplementary Tables S3, S4. Body weight, organ weight, and colon length were not significantly different between the experimental and control groups (Figures 9A–D). The organs exhibited no obvious pathological damage such as necrosis, inflammation, or proliferation (Figure 9E). All hematological parameters in the mice were comparable between the groups (Supplementary Table S5). There were no significant differences between the experimental and control groups in terms of alanine aminotransferase, aspartate aminotransferase, γ -glutamyltransferase, total bile acid, and creatinine (Table 4). Notably, serum uric acid levels in the experimental group were significantly lower than those in the

control group, suggesting that *R. intestinalis* may affect purine and uric acid metabolism. Based on these results, we determined that oral *R. intestinalis* has an LD₅₀ exceeding 1.9×10^9 CFU/kg.

28-day repeated dose study

No deaths or dosing-related adverse reactions were observed at any dose level during the 28-day experimental period. The average daily food and water intake is presented in Supplementary Tables S6, S7. Body weight, organ weight, and colon length did not differ significantly between groups (Figures 10A–D). No obvious pathological changes, such as necrosis, inflammation, or proliferation, were observed in the organs (Figure 10E). The hematological parameters did not differ significantly among the groups (Supplementary Table S8). In terms of alanine aminotransferase (ALT), aspartate aminotransferase (AST), alkaline phosphatase (ALP), γ -glutamyltransferase (γ -GT), total bile acid (TBA), and urea levels (Table 5), no significant differences were observed between the groups. Notably, the serum uric acid level in the experimental group was significantly lower than that in the control group, in agreement with the results of the acute oral toxicity test. Based on these data, the NOAEL for the oral administration of *R. intestinalis* was estimated at 1.32×10^9 CFU/kg/day for 28 days.

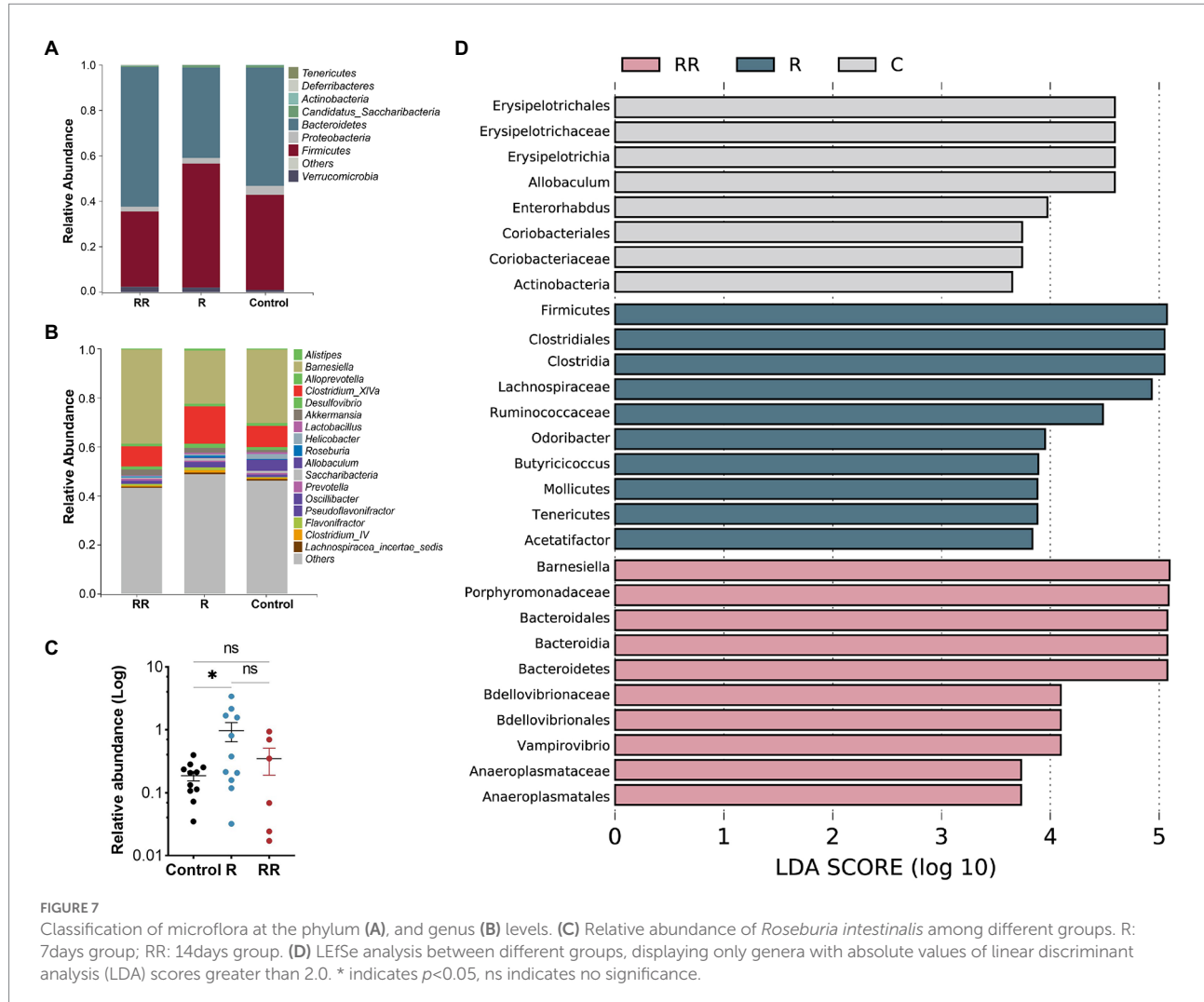


FIGURE 7

Classification of microflora at the phylum (A), and genus (B) levels. (C) Relative abundance of *Roseburia intestinalis* among different groups. R: 7days group; RR: 14days group. (D) LEfSe analysis between different groups, displaying only genera with absolute values of linear discriminant analysis (LDA) scores greater than 2.0. * indicates $p < 0.05$, ns indicates no significance.

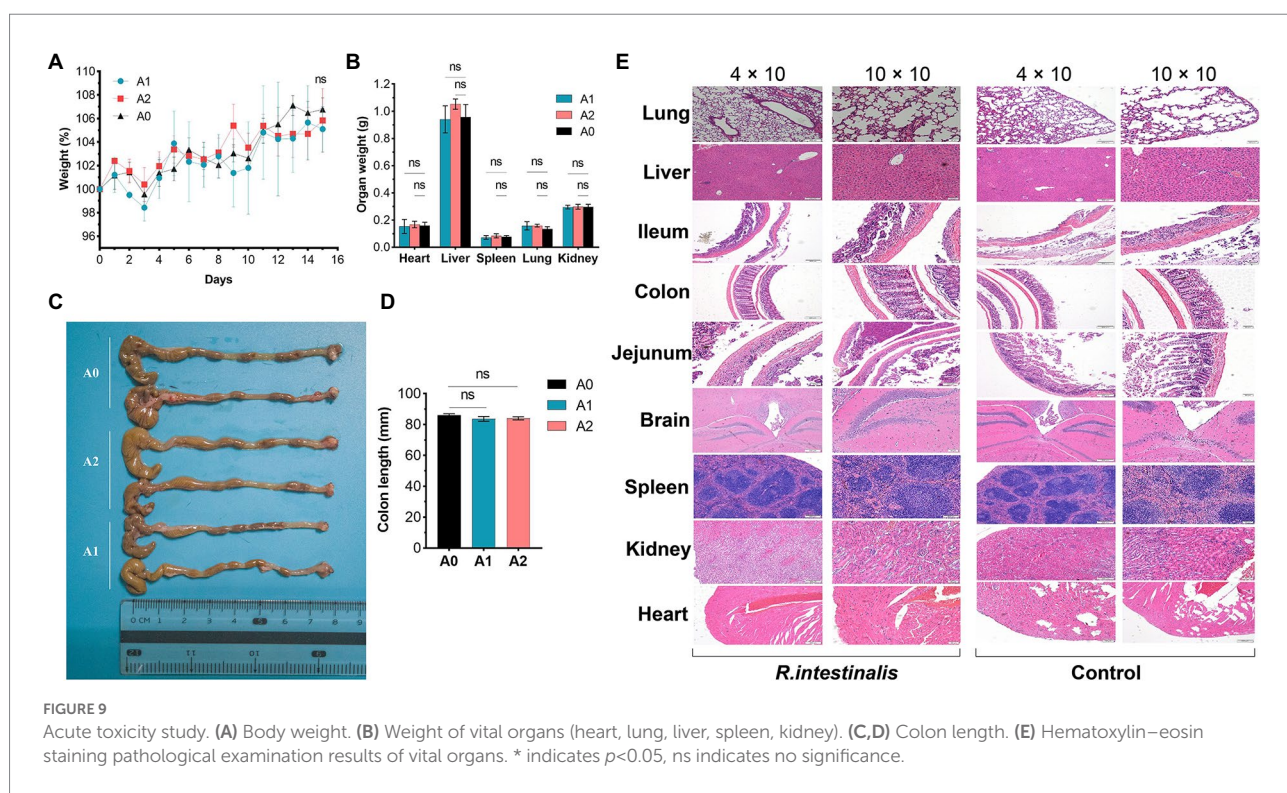
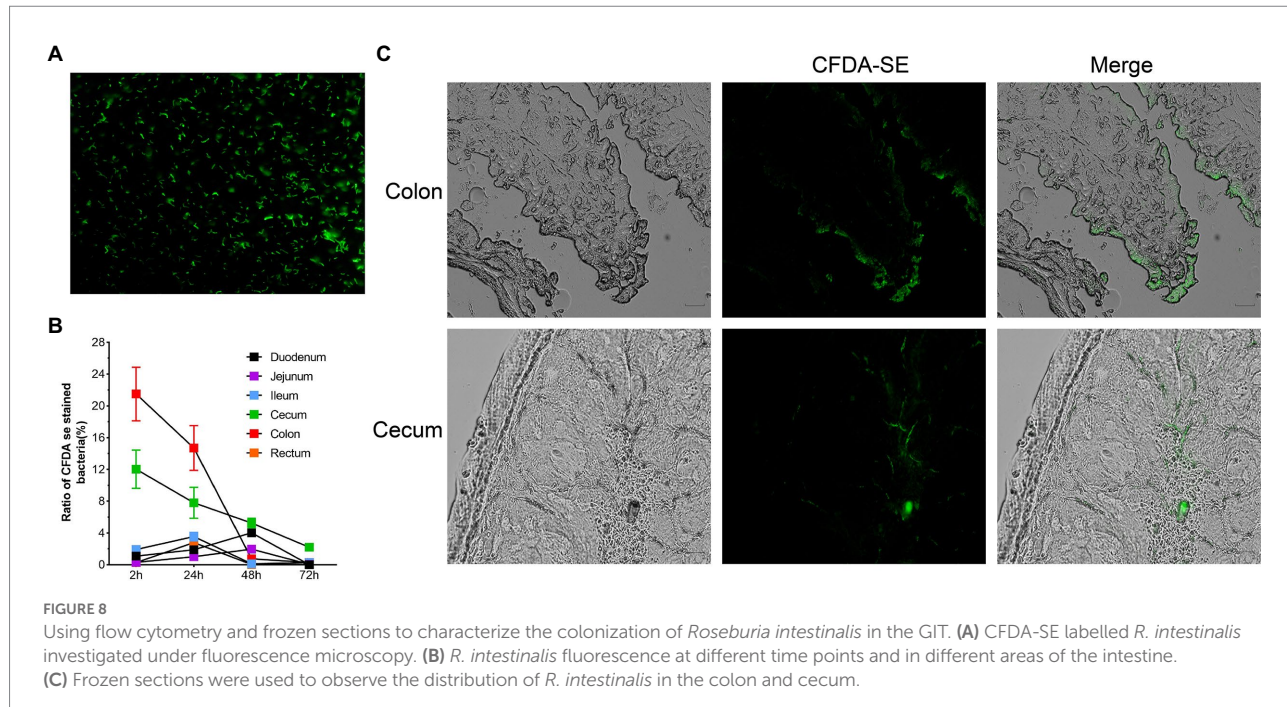
Discussion

Genomic, phenotypic, and oral safety studies should be conducted on potential probiotic strains to assess their safety and feasibility for industrial use.

A few virulence factors (VFs) have also been found in the genomes of nonpathogenic bacteria (Niu et al., 2013). Certain VFs are involved in host–microbe interactions, while others are involved in cell adhesion and host defense (Li et al., 2018). VF genes found in the *R. intestinalis* genome were related to adhesion (*fbpA/fbp68*, *ebpC*, *efaA*, *plr/gapA*) and lipid and fatty acid metabolism (*panD*). *FbpA* may play a role in the prevention of pathogenic colonization by inhibiting biofilm formation (Wang et al., 2017). *EfaA* is associated with adhesion of probiotics bacteria to both biotic and abiotic surfaces (Choeisoongnern et al., 2021). *GroEL* may inhibit colitis by inhibiting pro-inflammatory M1 macrophages and promoting the secretion of anti-inflammatory cytokines (Dias et al., 2021). The genome contains two tetracycline resistance genes, but a subsequent antibiotic susceptibility test showed that

R. intestinalis was susceptible to tetracycline. Gene modifications or pseudogenes may have causes this seemingly paradoxical result. Additionally, the expression of these genes may usually be low or they are induced only under specific circumstances, such as stimuli or signals from the environment (Li et al., 2018). Therefore, the presence of these resistance genes does not hinder the safety of *R. intestinalis* as a probiotic.

The CRISPR-Cas system is considered an defense mechanism against mobile genetic elements (Holy et al., 2020). This system can protect against re-invasion by capturing and integrating foreign nucleic acid fragments from the initial invasion. CRISPR-Cas genes have also been found in some probiotics, such as *Bifidobacterium* (Pan et al., 2020) and *Lactobacillus reuteri* (Alayande et al., 2020). Amino acids can be converted to biogenic amines via microbial decarboxylation. Histamine and tyramine (Zhu et al., 2020) are prevalent in fermented foods, and the excessive intake of biogenic amines can be harmful. The *R. intestinalis* genome contained genes involved in spermidine biosynthesis. Spermidine improves gut



barrier integrity (Ma et al., 2020b), reduces obesity and cancer mortality, and provides anti-inflammatory and stem cell senescence protection (Madeo et al., 2018). Probiotics, including *Akkermansia muciniphila*, may have anti-aging and anti-obesity effects, that are linked to increased levels of spermidine in the host (Grajeda-Iglesias et al., 2021).

Microbes in the gut synthesize several vitamins and essential amino acids that contribute to the host amino acid homeostasis (Gill et al., 2006; Lin et al., 2017). *R. intestinalis* contains genes for the biosynthesis of five essential amino acids and five vitamins. Prophages are generally considered beneficial to their bacterial hosts, especially in the gastrointestinal environment (Manrique et al.,

2017). The presence of prophages not only increases genetic variability but may also allow bacteria to cope with adverse environmental conditions (Casjens, 2003). Several probiotics contain prophages, including *Lactococcus*, *Bifidobacterium*, *Lactobacillus* (Pei et al., 2021), and *L. rhamnosus* (Brandt et al., 2001). Additionally, studies have suggested that prophages are present in more than 92% of *Lactobacillus* genomes (Sun et al., 2015). Jeffrey et al. (Cornuault et al., 2020) identified two active prophages in the genome of *R. intestinalis* and demonstrated that these prophages can influence short-term changes in the gut microbiota composition.

Bacteriocins are products synthesized by bacterial ribosomes that possess bacteriostatic properties (Deraz et al., 2005). Increasing antibiotic resistance has prompted researchers to focus on bacteriocins, since these may serve as alternatives to antibiotics (Cotter et al., 2013). *R. intestinalis* can produce Zoocin A, a 30 kDa D-alanyl-L-alanine endopeptidase bacteriocin that inhibits

streptococcal growth by binding and cleaving bacterial peptidoglycan (Gargis et al., 2009). *L. plantarum* (Seddik et al., 2017) and *Enterococcus* spp. (Ben Braïk and Smaoui, 2019) are two probiotics microbes known to produce bacteriocins. *R. intestinalis* contains four short-chain fatty acid (SCFA) synthesis gene clusters, including a butyrate synthesis gene cluster. Butyrate has several beneficial effects, including as an energy source for colonic epithelial cells and exerting anti-inflammatory properties by inhibiting nuclear factor (NF)- κ B (Segain et al., 2000). *Clostridium butyricum*, a butyrate-producing probiotic, inhibits intestinal tumor growth by modulating the Wnt pathway and gut microbiota (Chen et al., 2020). Moreover, VSL#3 modulates the gut microbiota-SCFA-hormone axis to combat obesity and diabetes (Yadav et al., 2013).

As the human genome encodes only approximately 17 carbohydrate-degrading enzymes, those produced by gut bacteria play a critical role in carbohydrate degradation (Bhattacharya et al., 2015). *R. intestinalis* contains 222 carbohydrate metabolism-related genes that likely play important roles in host carbohydrate metabolism. Maria et al. (Leth et al., 2020) demonstrated that *R. intestinalis* expresses RiCBM86, an enzyme that binds and absorbs xylan in the gut, reduces inflammation, and improves atherosclerosis (Kasahara et al., 2018). This bacterium is also a major degrader of β -mannans (La Rosa et al., 2019) and can produce xylanase to degrade xylan (Mirande et al., 2010). GIs are an important aspect of horizontal gene transfer and can transmit antibiotic resistance and virulence genes (Juhas et al., 2009). *R. intestinalis* contains 41 GIs, none of which contain virulence, antibiotic resistance, or pathogenicity genes.

Although the gastric juice pH is 1–3, it increases to 6 after food ingestion (De Angelis et al., 2006). The pH values of the duodenum, terminal ileum, cecum, and rectum are 6.0, 7.4, 5.7, and 6.7, respectively (Fallingborg, 1999). Several methods have been reported for enhancing the tolerance of probiotics to bile

TABLE 4 Clinical chemistry results of acute toxicity study.

<i>R. intestinalis</i>	Control	P
ALT (U/L)	41.29 ± 8.1	0.420
ALP (U/L)	136.73 ± 17.32	0.105
AST (U/L)	121.44 ± 18.89	0.667
γ -GT (U/L)	0.89 ± 0.85	0.744
UREA (mg/dL)	32.35 ± 2.35	0.317
CREA (umol/L)	13.14 ± 0.81	0.330
DBIL (umol/L)	4.04 ± 0.41	0.439
TBA (umol/L)	3.27 ± 0.34	0.443
UA (umol/L)	75.58 ± 1.62	0.035
TBIL (umol/L)	8.33 ± 0.68	0.549

ALT: Alanine aminotransferase; AST: Aspartate aminotransferase; ALP: alkaline phosphatase; γ -GT: γ -glutamyltransferase; DBIL: Direct Bilirubin; TBA: total bile acid; TBIL: total bilirubin; UA: uric acid.

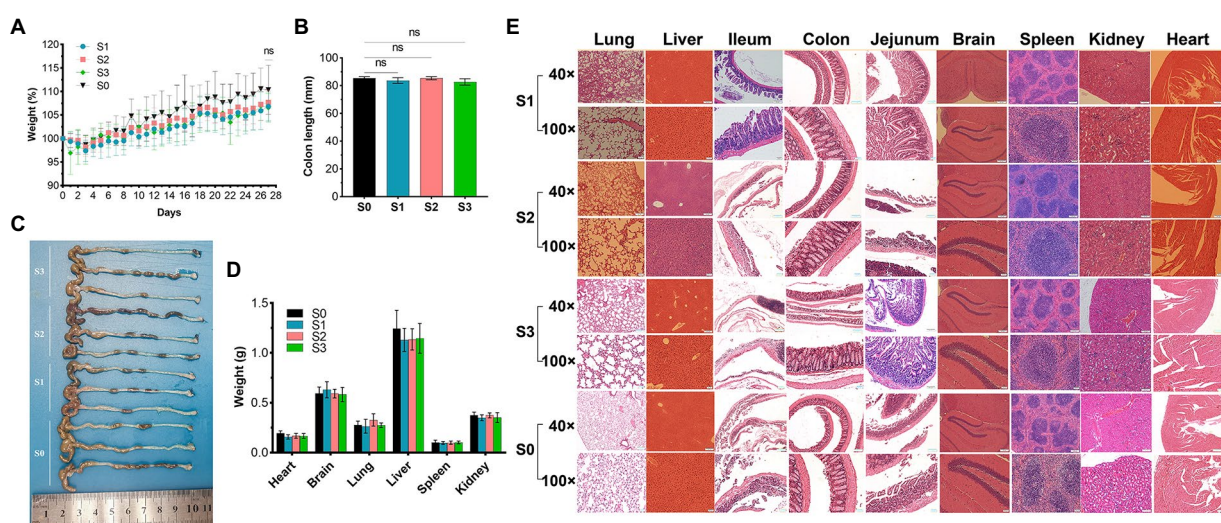


FIGURE 10
28-Day repeated dose study. (A) Body weight. (B,C) Colon length. (D) Weight of vital organs (heart, lung, brain, liver, spleen, kidney). (E) Hematoxylin–eosin staining pathological examination of organs. * indicates $p < 0.05$, ns indicates no significance.

TABLE 5 Clinical chemistry results of 28-day repeated dose study.

	S0	S1	S2	S3	P
AST (U/L)	176.06 ± 57.97	229.68 ± 103.16	149.19 ± 23.92	145.71 ± 46.66	0.28
ALT (U/L)	42.06 ± 12.43	33.92 ± 4.48	36.4 ± 8.89	49.5 ± 11.26	0.17
DBIL (umol/L)	3.99 ± 0.75	5.11 ± 1.72	3.66 ± 0.39	3.91 ± 1.19	0.32
TBIL (umol/L)	11.02 ± 1.55	8.73 ± 1.01	8.35 ± 0.98	9.35 ± 1.45	0.05
ALP (U/L)	154.2 ± 19.17	140.39 ± 25.04	164.5 ± 29.73	140.22 ± 26.72	0.49
γGT (U/L)	1.92 ± 1.37	2.26 ± 0.83	2.62 ± 2.86	2.12 ± 0.5	0.94
TBA (umol/L)	4.73 ± 1.46	22.88 ± 36.04	6.38 ± 4.6	4.73 ± 3.31	0.45
UREA (umol/L)	26.4 ± 1.97	23.6 ± 3.19	25.07 ± 1.36	25.81 ± 2.64	0.42
CREA (umol/L)	26.83 ± 0.51	25.85 ± 1.75	23.98 ± 2.56	29.14 ± 6.19	0.26
UA (umol/L)	115.93 ± 36.31	107.9 ± 17.82	69.49 ± 13.33	69.66 ± 22.83	0.03

salts and acids. Gou et al. (2021) used soybean lecithin and whey protein concentrate to treat *Lacticaseibacillus paracasei* and successfully increased its tolerance to bile salts and acids. Evidence suggests that 5% lactose can enhance the bile salt tolerance of *L. bulgaricus* (Mena and Aryana, 2018), whereas soy lecithin (Hu et al., 2015) can enhance the bile salt resistance of *L. plantarum* and whey protein (Vargas et al., 2015) can enhance the acid and bile salt tolerance of *Streptococcus thermophilus*. Biofilm formation by probiotics can inhibit pathogens from colonizing the mucosa (Deng et al., 2020). *R. intestinalis* forms a higher percentage of biofilms than many common probiotics and pathogenic bacteria, further highlighting its probiotic properties.

Following the administration of *R. intestinalis*, the serum uric acid level decreased significantly, suggesting that the bacterium may influence the host's purine and uric acid metabolism. Our *in vitro* study indicates that *R. intestinalis* can degrade 60% of the uric acid in the surrounding environment within 24 h (data not shown), although further investigation is required to determine the underlying mechanism.

R. intestinalis did not adversely affect the abundance or variety of the gut flora. After 14 days of continuous administration, the relative abundance of *R. intestinalis* did not increase proportionally. However, the structure of the flora changed, and the predominant flora consisted of *Barnesiella* and *porphyromonadaceae*. The relative abundance of *R. intestinalis* was determined by 16S rRNA sequencing of stool samples. Owing to their ease of collection, feces are often used to study the gut microbiota. Nonetheless, this method has a limited ability to detect the mucosal-associated microbiota. Mucosal-associated microbiota and luminal microbiota have only a partial association (Zmora et al., 2018). Due to their biofilm-like

structure, mucosal-associated microbiota promote beneficial functions in intestinal epithelial cells (Sonnenburg et al., 2004), and conventional sampling methods (feces or intestinal tissue) may underestimate their levels (Donaldson et al., 2016). *R. intestinalis* adheres to the intestinal mucosa and colonizes the cecum and colonic mucosa. Flow cytometry results showed that there was a low abundance of *R. intestinalis* in the intestinal contents (Figure 8B). Similarly, some probiotics, such as *B. lactis*, showed a decreasing trend in its levels after prolonged administration (Ma et al., 2020a). Therefore, we speculated that the variation in the gut flora is stratified rather than continuous, and a relatively balanced state of host-microbe symbiosis exists in the gut microbiota (Arumugam et al., 2011). Studies indicate that the gut microbiota is partially stable, with approximately 40 species of bacteria forming a core microbiota that persists in humans for at least 1 year (Donaldson et al., 2016). Additionally, mucosal flora analysis revealed an increase in *Enterobacteriaceae* and a decrease in *Clostridium* in patients with Crohn's disease. However, these features disappeared when stool samples were examined (Gevers et al., 2014).

Probiotics may have an impact on the host even though they do not necessarily interact with indigenous microbiota (Hill et al., 2014). Instead, they may normalize the disturbed microbiota and modulate it in a beneficial manner. It is difficult to identify patterns of change in commonly altered microbes among studies that report probiotic-associated microbiome alterations. The average relative abundance of *R. intestinalis* in healthy individuals is estimated at only 0.09377% according to the Gmrepo database (Dai et al., 2022). Thus, *R. intestinalis* is not predominant in the entire intestinal flora composition. This may explain why, after taking *R. intestinalis* for a short period, it remains difficult for the bacterium to become the predominant. A clinical study also found that after administration *L. paracasei* DG, the α-diversity of the intestinal flora did not change, but the β-diversity and structure changed (Ferrario et al., 2014) with an increase in *Brucella* and *Faecalis*. Administration of *R. intestinalis* increased the levels of certain beneficial gut bacteria. *Porphyromonadaceae* abundance increased in long-lived populations, and the proportion of *R. intestinalis* also increased (Ren et al., 2021). The abundance of *Barnesiella*, *Porphyromonadaceae*, and *Roseburia* also increased after vitamin D1 administration in patients with Crohn's disease (Schäffler et al., 2018), indicating that these bacteria may function synergistically. In addition to its resistance to IBD (Weiss et al., 2014), *Barnesiella* is a valuable "oncomicrobiotic" for antitumor immunomodulator therapy (Daillère et al., 2016). *Barnesiella* has also been associated with remission from obesity and hepatic steatosis (Rodriguez et al., 2020) and with the clearance of vancomycin-resistant *Enterococcus* in the gut (Ubeda et al., 2013). *Porphyromonadaceae* has been associated with reduced visceral fat and a healthier metabolic profile in the elderly (Tavella et al., 2021). Therefore, the probiotic effect of *R. intestinalis* may be that it constitutes an interaction network with several beneficial gut microbes, such as *Barnesiella* and *Porphyromonadaceae*.

CFDA-SE is a fluorescent dye with many advantages such as strong fluorescence, low toxicity, and good stability. Several

researchers (Lee et al., 2004; Wang et al., 2019, 2021; Zhao et al., 2022) have used this method to tag and track bacteria. *R. intestinalis* was detected in all intestinal sites 2 h after administration, whereas after 48 h, *R. intestinalis* was predominantly located in the cecum, and not present in the colon. This distribution may be related to the physiology of the different parts of the gut (Donaldson et al., 2016; Martinez-Guryn et al., 2019). Using frozen section analysis, we observed that *R. intestinalis* colonizing the cecum and mucus layer of the colon. Abbeele et al. demonstrated that *R. intestinalis* colonized the mucin layer using *in vitro* intestinal models (Van den Abbeele et al., 2013), which corresponds with our observations *in vivo*.

Conclusion

In conclusion, we performed a comprehensive safety assessment of *R. intestinalis*. An *in vitro* study and genomic analysis revealed that *R. intestinalis* was not cytotoxic and caused no safety concerns associated with antibiotic resistance genes, virulence factors, biogenic amine production, gelatinase, or DNase activity. *In vivo* experiments showed that orally administrated *R. intestinalis* mainly colonizes the cecum and colonic mucus layers without altering the abundance and diversity of the gut microbiota. An oral toxicity study conducted in mice revealed that *R. intestinalis* was not toxic and could reduce serum uric acid levels. This study highlights *R. intestinalis* as a non-pathogenic strain suitable for use as a “Next Generation Probiotic.”

Data availability statement

The raw sequences generated for this study can be found in the NCBI Short Read Archive under BioProject no. PRJNA850191.

Ethics statement

The animal study was reviewed and approved by Central South University Animal Ethics Committee (XMSB-2022-0198).

References

- Alayande, K. A., Aiyejoro, O. A., Nengwekhulu, T. M., Katata-Seru, L., and Ateba, C. N. (2020). Integrated genome-based probiotic relevance and safety evaluation of lactobacillus reuteri PNW1. *PLoS One* 15:e0235873. doi: 10.1371/journal.pone.0235873
- Alcock, B. P., Raphenya, A. R., Lau, T. T. Y., Tsang, K. K., Bouchard, M., Edalatmand, A., et al. (2020). CARD 2020: antibiotic resistome surveillance with the comprehensive antibiotic resistance database. *Nucleic Acids Res.* 48, D517–D525. doi: 10.1093/nar/gkz935
- Alikhan, N. F., Petty, N. K., Ben Zakour, N. L., and Beatson, S. A. (2011). BLAST ring image generator (BRIG): simple prokaryote genome comparisons. *BMC Genomics* 12, 402. doi: 10.1186/1471-2164-12-402
- Anandharaj, M., Sivasankari, B., Santhanakaruppu, R., Manimaran, M., Rani, R. P., and Sivakumar, S. (2015). Determining the probiotic potential of cholesterol-reducing lactobacillus and Weissella strains isolated from gherkins (fermented cucumber) and south Indian fermented koozh. *Res. Microbiol.* 166, 428–439. doi: 10.1016/j.resmic.2015.03.002
- Arndt, D., Grant, J. R., Marcu, A., Sajed, T., Pon, A., Liang, Y., et al. (2016). PHASTER: a better, faster version of the PHAST phage search tool. *Nucleic Acids Res.* 44, W16–W21. doi: 10.1093/nar/gkw387
- Arumugam, M., Raes, J., Pelletier, E., Le Paslier, D., Yamada, T., Mende, D. R., et al. (2011). Enterotypes of the human gut microbiome. *Nature* 473, 174–180. doi: 10.1038/nature09944
- Ben Braïek, O., and Smaoui, S. (2019). Enterococci: Between emerging pathogens and potential probiotics. *Biomed. Res. Int.* 2019, 1–13. doi: 10.1155/2019/5938210
- Bertelli, C., Laird, M. R., Williams, K. P., Lau, B. Y., Hoad, G., Winsor, G. L., et al. (2017). IslandViewer 4: expanded prediction of genomic islands for larger-scale datasets. *Nucleic Acids Res.* 45, W30–w35. doi: 10.1093/nar/gkx343

Author contributions

CZ analyzed the strain phenotypically and genetically and drafted the manuscript. KM and KN helped with genomic and bioinformatic analyses. WL and XinW contributed to the phenotypic experiments. YH helped to carry out the experiments on mice and fluorescently label of bacteria. MD contributed to revising the manuscript. XiaW oversaw the project and reviewed and revised the manuscript. All authors contributed to the article and approved the submitted version.

Funding

This project was supported by the National Natural Science Foundation of China (NSFC no. 81970494).

Conflict of interest

The authors declare that the research was conducted in the absence of any commercial or financial relationships that could be construed as a potential conflict of interest.

Publisher's note

All claims expressed in this article are solely those of the authors and do not necessarily represent those of their affiliated organizations, or those of the publisher, the editors and the reviewers. Any product that may be evaluated in this article, or claim that may be made by its manufacturer, is not guaranteed or endorsed by the publisher.

Supplementary material

The Supplementary material for this article can be found online at: <https://www.frontiersin.org/articles/10.3389/fmicb.2022.973046/full#supplementary-material>

- Bhattacharya, T., Ghosh, T. S., and Mande, S. S. (2015). Global profiling of carbohydrate active enzymes in human gut microbiome. *PLoS One* 10:e0142038. doi: 10.1371/journal.pone.0142038
- Brandt, K., Tilsala-Timisjärvi, A., and Alatossava, T. (2001). Phage-related DNA polymorphism in dairy and probiotic lactobacillus. *Micron* 32, 59–65. doi: 10.1016/S0968-4328(00)00030-5
- Casjens, S. (2003). Prophages and bacterial genomics: what have we learned so far? *Mol. Microbiol.* 49, 277–300. doi: 10.1046/j.1365-2958.2003.03580.x
- Chen, D., Jin, D., Huang, S., Wu, J., Xu, M., Liu, T., et al. (2020). Clostridium butyricum, a butyrate-producing probiotic, inhibits intestinal tumor development through modulating Wnt signaling and gut microbiota. *Cancer Lett.* 469, 456–467. doi: 10.1016/j.canlet.2019.11.019
- Choeisoongnern, T., Sirilun, S., Waditee-Sirisattha, R., Pintha, K., Peerajan, S., and Chaiyasut, C. (2021). Potential probiotic enterococcus faecium OV3-6 and its bioactive peptide as alternative bio-preservation. *Foods* 10:2264. doi: 10.3390/foods10102264
- CLSI. (2016). “Performance standards for antimicrobial susceptibility testing,” in *CLSI Document M100S. 26th Edn.* (Wayne, PA: Clinical and Laboratory Standards Institute).
- Cornuault, J. K., Moncaut, E., Loux, V., Mathieu, A., Sokol, H., Petit, M. A., et al. (2020). The enemy from within: a prophage of Roseburia intestinalis systematically turns lytic in the mouse gut, driving bacterial adaptation by CRISPR spacer acquisition. *ISME J.* 14, 771–787. doi: 10.1038/s41396-019-0566-x
- Cotter, P. D., Ross, R. P., and Hill, C. (2013). Bacteriocins - a viable alternative to antibiotics? *Nat. Rev. Microbiol.* 11, 95–105. doi: 10.1038/nrmicro2937
- Couvin, D., Bernheim, A., Toffano-Nioche, C., Touchon, M., Michalik, J., Néron, B., et al. (2018). CRISPRCasFinder, an update of CRISPRFinder, includes a portable version, enhanced performance and integrates search for Cas proteins. *Nucleic Acids Res.* 46, W246–w251. doi: 10.1093/nar/gky425
- Cozzolino, A., Vergalito, F., Tremonte, P., Iorizzo, M., Lombardi, S. J., Sorrentino, E., et al. (2020). Preliminary evaluation of the safety and probiotic potential of Akkermansia muciniphila DSM 22959 in comparison with lactobacillus rhamnosus GG. *Microorganisms* 8:189. doi: 10.3390/microorganisms8020189
- Dai, D., Zhu, J., Sun, C., Li, M., Liu, J., Wu, S., et al. (2022). GMrepo v2: a curated human gut microbiome database with special focus on disease markers and cross-dataset comparison. *Nucleic Acids Res.* 50, D777–d784. doi: 10.1093/nar/gkab1019
- Daillère, R., Vétizou, M., Waldschmitt, N., Yamazaki, T., Isnard, C., Poirier-Colame, V., et al. (2016). Enterococcus hirae and Barnesiella intestinihominis facilitate cyclophosphamide-induced therapeutic Immunomodulatory effects. *Immunity* 45, 931–943. doi: 10.1016/j.immuni.2016.09.009
- Davis, J. J., Wattam, A. R., Aziz, R. K., Brettin, T., Butler, R., Butler, R. M., et al. (2020). The PATRIC bioinformatics resource center: expanding data and analysis capabilities. *Nucleic Acids Res.* 48, D606–d612. doi: 10.1093/nar/gkz943
- De Angelis, M., Rizzello, C. G., Fasano, A., Clemente, M. G., De Simone, C., Silano, M., et al. (2006). VSL#3 probiotic preparation has the capacity to hydrolyze gliadin polypeptides responsible for celiac Sprue. *Biochim. Biophys. Acta* 1762, 80–93. doi: 10.1016/j.bbadiis.2005.09.008
- Deng, Z., Luo, X. M., Liu, J., and Wang, H. (2020). Quorum sensing, biofilm, and intestinal mucosal barrier: involvement the role of probiotic. *Front. Cell. Infect. Microbiol.* 10:538077. doi: 10.3389/fcimb.2020.538077
- Deraz, S. F., Karlsson, E. N., Hedström, M., Andersson, M. M., and Mattiasson, B. (2005). Purification and characterisation of acidocin D20079, a bacteriocin produced by lactobacillus acidophilus DSM 20079. *J. Biotechnol.* 117, 343–354. doi: 10.1016/j.jbiotec.2005.02.005
- Devaux, C. A., Million, M., and Raoult, D. (2020). The Butyrogenic and lactic bacteria of the gut microbiota determine the outcome of Allogenic hematopoietic cell transplant. *Front. Microbiol.* 11:1642. doi: 10.3389/fmicb.2020.01642
- Dias, A. M. M., Douhard, R., Hermetet, F., Regimbeau, M., Lopez, T. E., Gonzalez, D., et al. (2021). Lactobacillus stress protein GroEL prevents colonic inflammation. *J. Gastroenterol.* 56, 442–455. doi: 10.1007/s00535-021-01774-3
- Dillon, S. M., Kibbie, J., Lee, E. J., Guo, K., Santiago, M. L., Austin, G. L., et al. (2017). Low abundance of colonic butyrate-producing bacteria in HIV infection is associated with microbial translocation and immune activation. *AIDS* 31, 511–521. doi: 10.1097/QAD.00000000000001366
- Donaldson, G. P., Lee, S. M., and Mazmanian, S. K. (2016). Gut biogeography of the bacterial microbiota. *Nat. Rev. Microbiol.* 14, 20–32. doi: 10.1038/nrmicro3552
- Drula, E., Garron, M.-L., Dogan, S., Lombard, V., Henrissat, B., and Terrapon, N. (2021). The carbohydrate-active enzyme database: functions and literature. *Nucleic Acids Res.* 50, D571–D577. doi: 10.1093/nar/gkab1045
- Dudík, B., Kiňová Sepová, H., Bilka, F., Pašková, L., and Bilková, A. (2020). Mucin pre-cultivated lactobacillus reuteri E shows enhanced adhesion and increases mucin expression in HT-29 cells. *Antonie Van Leeuwenhoek* 113, 1191–1200. doi: 10.1007/s10482-020-01426-1
- Duncan, S. H., Hold, G. L., Barcenilla, A., Stewart, C. S., and Flint, H. J. (2002). Roseburia intestinalis sp. nov., a novel saccharolytic, butyrate-producing bacterium from human faeces. *Int. J. Syst. Evol. Microbiol.* 52, 1615–1620. doi: 10.1099/00207713-52-5-1615
- Fallingborg, J. (1999). Intraluminal pH of the human gastrointestinal tract. *Dan. Med. Bull.* 46, 183–196. PMID: 10421978
- Fan, H., Chen, Z., Lin, R., Liu, Y., Wu, X., Puthiyakunnon, S., et al. (2019). Bacteroides fragilis strain ZY-312 defense against Cronobacter sakazakii-induced necrotizing Enterocolitis In vitro and in a neonatal rat model. *mSystems* 4:19. doi: 10.1128/mSystems.00305-19
- Ferrario, C., Taverniti, V., Milani, C., Fiore, W., Laureati, M., De Noni, I., et al. (2014). Modulation of fecal Clostridiales bacteria and butyrate by probiotic intervention with lactobacillus paracasei DG varies among healthy adults. *J. Nutr.* 144, 1787–1796. doi: 10.3945/jn.114.197723
- Gargis, S. R., Heath, H. E., Heath, L. S., Leblanc, P. A., Simmonds, R. S., Abbott, B. D., et al. (2009). Use of 4-sulfophenyl isothiocyanate labeling and mass spectrometry to determine the site of action of the streptococcal peptidoglycan hydrolase zocin A. *Appl. Environ. Microbiol.* 75, 72–77. doi: 10.1128/AEM.01647-08
- Gevers, D., Kugathasan, S., Denzon, L. A., Vázquez-Baeza, Y., Van Treuren, W., Ren, B., et al. (2014). The treatment-naïve microbiome in new-onset Crohn's disease. *Cell Host Microbe* 15, 382–392. doi: 10.1016/j.chom.2014.02.005
- Gill, S. R., Pop, M., Deboy, R. T., Eckburg, P. B., Turnbaugh, P. J., Samuel, B. S., et al. (2006). Metagenomic analysis of the human distal gut microbiome. *Science* 312, 1355–1359. doi: 10.1126/science.1124234
- Gou, X., Zhang, L., Zhao, S., Ma, W., and Yang, Z. (2021). Application of the combination of soybean lecithin and whey protein concentrate 80 to improve the bile salt and acid tolerance of probiotics. *J. Microbiol. Biotechnol.* 31, 840–846. doi: 10.4014/jmb.2103.03017
- Grajeda-Iglesias, C., Durand, S., Daillère, R., Iribarren, K., Lemaitre, F., Derosa, L., et al. (2021). Oral administration of Akkermansia muciniphila elevates systemic antiaging and anticancer metabolites. *Aging (Albany NY)* 13, 6375–6405. doi: 10.18632/aging.202739
- Hill, C., Guarner, F., Reid, G., Gibson, G. R., Merenstein, D. J., Pot, B., et al. (2014). Expert consensus document. The international scientific Association for Probiotics and Prebiotics consensus statement on the scope and appropriate use of the term probiotic. *Nat. Rev. Gastroenterol. Hepatol.* 11, 506–514. doi: 10.1038/nrgastro.2014.66
- Holý, O., Parra-Flores, J., Lepuschitz, S., Alarcón-Lavín, M. P., Cruz-Córdova, A., Xicotencatl-Cortes, J., et al. (2020). Molecular characterization of Cronobacter sakazakii strains isolated from powdered Milk. *Foods* 10:20. doi: 10.3390/foods10010020
- Hu, B., Tian, F., Wang, G., Zhang, Q., Zhao, J., Zhang, H., et al. (2015). Enhancement of bile resistance in lactobacillus plantarum strains by soy lecithin. *Lett. Appl. Microbiol.* 61, 13–19. doi: 10.1111/lam.12418
- Hussein, W. E., Abdelhamid, A. G., Rocha-Mendoza, D., García-Cano, I., and Yousef, A. E. (2020). Assessment of safety and probiotic traits of enterococcus durans OSY-EGY, isolated From Egyptian artisanal cheese, using comparative genomics and phenotypic analyses. *Front. Microbiol.* 11:608314. doi: 10.3389/fmicb.2020.608314
- Juhás, M., van der Meer, J. R., Gaillard, M., Harding, R. M., Hood, D. W., and Crook, D. W. (2009). Genomic islands: tools of bacterial horizontal gene transfer and evolution. *FEMS Microbiol. Rev.* 33, 376–393. doi: 10.1111/j.1574-6976.2008.00136.x
- Kasahara, K., Krautkramer, K. A., Org, E., Romano, K. A., Kerby, R. L., Vivas, E. I., et al. (2018). Interactions between Roseburia intestinalis and diet modulate atherosclerosis in a murine model. *Nat. Microbiol.* 3, 1461–1471. doi: 10.1038/s41564-018-0272-x
- La Rosa, S. L., Leth, M. L., Michalak, L., Hansen, M. E., Pudlo, N. A., Glowacki, R., et al. (2019). The human gut Firmicute Roseburia intestinalis is a primary degrader of dietary β-mannans. *Nat. Commun.* 10, 905. doi: 10.1038/s41467-019-08812-y
- Lee, S. E., Choi, Y., Jun, J. E., Lee, Y. B., Jin, S. M., Hur, K. Y., et al. (2019). Additional effect of dietary fiber in patients with type 2 diabetes mellitus using metformin and sulfonylurea: An open-label. *Pilot Trial. Diabetes Metab J* 43, 422–431. doi: 10.4093/dmj.2018.0090
- Lee, Y. K., Ho, P. S., Low, C. S., Arvilommi, H., and Salminen, S. (2004). Permanent colonization by lactobacillus casei is hindered by the low rate of cell division in mouse gut. *Appl. Environ. Microbiol.* 70, 670–674. doi: 10.1128/AEM.70.2.670-674.2004
- Leth, M. L., Ejby, M., Madland, E., Kitaoku, Y., Slotboom, D. J., Guskov, A., et al. (2020). Molecular insight into a new low-affinity xylan binding module from the xylanolytic gut symbiont Roseburia intestinalis. *FEBS J.* 287, 2105–2117. doi: 10.1111/febs.15117

- Li, Q., Hu, W., Liu, W. X., Zhao, L. Y., Huang, D., Liu, X. D., et al. (2021). *Streptococcus thermophilus* inhibits colorectal tumorigenesis Through secreting β -Galactosidase. *Gastroenterology* 160, 1179–1193.e14. doi: 10.1053/j.gastro.2020.09.003
- Li, B., Zhan, M., Evivie, S. E., Jin, D., Zhao, L., Chowdhury, S., et al. (2018). Evaluating the safety of potential probiotic *Enterococcus durans* KLDs6.0930 using whole genome sequencing and Oral toxicity study. *Front. Microbiol.* 9:1943. doi: 10.3389/fmicb.2018.01943
- Liang, Q., Chiu, J., Chen, Y., Huang, Y., Higashimori, A., Fang, J., et al. (2017). Fecal bacteria act as novel biomarkers for noninvasive diagnosis of colorectal cancer. *Clin. Cancer Res.* 23, 2061–2070. doi: 10.1158/1078-0432.CCR-16-1599
- Lin, R., Liu, W., Piao, M., and Zhu, H. (2017). A review of the relationship between the gut microbiota and amino acid metabolism. *Amino Acids* 49, 2083–2090. doi: 10.1007/s00726-017-2493-3
- Liu, S., Zhao, W., Liu, X., and Cheng, L. (2020). Metagenomic analysis of the gut microbiome in atherosclerosis patients identify cross-cohort microbial signatures and potential therapeutic target. *FASEB J.* 34, 14166–14181. doi: 10.1096/fj.202000622R
- Liu, B., Zheng, D., Zhou, S., Chen, L., and Yang, J. (2022). VFDB 2022: a general classification scheme for bacterial virulence factors. *Nucleic Acids Res.* 50, D912–D917. doi: 10.1093/nar/gkab1107
- Lu, W., Gao, B., Fan, J., Cheng, P., Hu, Y., Jie, Q., et al. (2019). Mesenchymal progenitors derived from different locations in long bones display diverse characteristics. *Stem Cells Int.* 2019, 1–11. doi: 10.1155/2019/5037578
- Luo, W., Shen, Z., Deng, M., Li, X., Tan, B., Xiao, M., et al. (2019). *Roseburia intestinalis* supernatant ameliorates colitis induced in mice by regulating the immune response. *Mol. Med. Rep.* 20, 1007–1016. doi: 10.3892/mmr.2019.10327
- Ma, C., Huo, D., You, Z., Peng, Q., Jiang, S., Chang, H., et al. (2020a). Differential pattern of indigenous microbiome responses to probiotic *Bifidobacterium lactis* V9 consumption across subjects. *Food Res. Int.* 136:109496. doi: 10.1016/j.foodres.2020.109496
- Ma, L., Ni, Y., Wang, Z., Tu, W., Ni, L., Zhuge, F., et al. (2020b). Spermidine improves gut barrier integrity and gut microbiota function in diet-induced obese mice. *Gut Microbes* 12, 1–19. doi: 10.1080/19490976.2020.1832857
- Machiels, K., Joossens, M., Sabino, J., De Preter, V., Arijs, I., Eeckhaut, V., et al. (2014). A decrease of the butyrate-producing species *Roseburia hominis* and *Faecalibacterium prausnitzii* defines dysbiosis in patients with ulcerative colitis. *Gut* 63, 1275–1283. doi: 10.1136/gutjnl-2013-304833
- Madeo, F., Eisenberg, T., Pietrocola, F., and Kroemer, G. (2018). Spermidine in health and disease. *Science* 359:2788. doi: 10.1126/science.aan2788
- Manrique, P., Dills, M., and Young, M. J. (2017). The human gut phage community and its implications for health and disease. *Viruses* 9:141. doi: 10.3390/v9060141
- Martinez-Guryn, K., Leone, V., and Chang, E. B. (2019). Regional diversity of the gastrointestinal microbiome. *Cell Host Microbe* 26, 314–324. doi: 10.1016/j.chom.2019.08.011
- Mena, B., and Aryana, K. (2018). Short communication: lactose enhances bile tolerance of yogurt culture bacteria. *J. Dairy Sci.* 101, 1957–1959. doi: 10.3168/jds.2017-13919
- Metlakunta, A. S., and Soman, R. J. (2020). Safety evaluation of *Bacillus coagulans* SNZ 1969 in Wistar rats. *Regul. Toxicol. Pharmacol.* 110:104538. doi: 10.1016/j.yrtph.2019.104538
- Miquel, S., Leclerc, M., Martin, R., Chain, F., Lenoir, M., Raguideau, S., et al. (2015). Identification of metabolic signatures linked to anti-inflammatory effects of *Faecalibacterium prausnitzii*. *MBio* 6:15. doi: 10.1128/mBio.00300-15
- Mirande, C., Kadlecikova, E., Matulova, M., Capek, P., Bernalier-Donadille, A., Forano, E., et al. (2010). Dietary fibre degradation and fermentation by two xylanolytic bacteria *Bacteroides xylanisolvens* XB1A and *Roseburia intestinalis* XB6B4 from the human intestine. *J. Appl. Microbiol.* 109, 451–460. doi: 10.1111/j.1365-2672.2010.04671.x
- Montalban-Arques, A., Katkeviciute, E., Busenhart, P., Bircher, A., Wirbel, J., Zeller, G., et al. (2021). Commensal Clostridiales strains mediate effective anti-cancer immune response against solid tumors. *Cell Host Microbe* 29, 1573–1588.e7. doi: 10.1016/j.chom.2021.08.001
- Nicholson, K., Bjornevik, K., Abu-Ali, G., Chan, J., Cortese, M., Dedi, B., et al. (2021). The human gut microbiota in people with amyotrophic lateral sclerosis. *Amyotroph Lateral Scler Frontotemporal Degener* 22, 186–194. doi: 10.1080/21678421.2020.1828475
- Nie, K., Ma, K., Luo, W., Shen, Z., Yang, Z., Xiao, M., et al. (2021). *Roseburia intestinalis*: A beneficial gut organism From the discoveries in genus and species. *Front. Cell. Infect. Microbiol.* 11:757718. doi: 10.3389/fcimb.2021.757718
- Niu, C., Yu, D., Wang, Y., Ren, H., Jin, Y., Zhou, W., et al. (2013). Common and pathogen-specific virulence factors are different in function and structure. *Virulence* 4, 473–482. doi: 10.4161/viru.25730
- O'Toole, P. W., Marchesi, J. R., and Hill, C. (2017). Next-generation probiotics: the spectrum from probiotics to live biotherapeutics. *Nat. Microbiol.* 2, 17057. doi: 10.1038/nmicrobiol.2017.57
- Overbeek, R., Olson, R., Pusch, G. D., Olsen, G. J., Davis, J. J., Disz, T., et al. (2014). The SEED and the rapid annotation of microbial genomes using subsystems technology (RAST). *Nucleic Acids Res.* 42, D206–D214. doi: 10.1093/nar/gkt1226
- Pan, X., Kaminga, A. C., Liu, A., Wen, S. W., Luo, M., and Luo, J. (2021). Gut microbiota, glucose, lipid, and water-electrolyte metabolism in children With nonalcoholic fatty liver disease. *Front. Cell. Infect. Microbiol.* 11:683743. doi: 10.3389/fcimb.2021.683743
- Pan, M., Nethery, M. A., Hidalgo-Cantabrana, C., and Barrangou, R. (2020). Comprehensive mining and characterization of CRISPR-Cas Systems in *Bifidobacterium*. *Microorganisms* 8:720. doi: 10.3390/microorganisms8050720
- Pascal Andreu, V., Roel-Touris, J., Dodd, D., Fischbach, M. A., and Medema, M. H. (2021). The gut SMASH web server: automated identification of primary metabolic gene clusters from the gut microbiota. *Nucleic Acids Res.* 49, W263–W270. doi: 10.1093/nar/gkab353
- Pei, Z., Sadiq, F. A., Han, X., Zhao, J., Zhang, H., Ross, R. P., et al. (2021). Comprehensive scanning of Prophages in *lactobacillus*: distribution, diversity, antibiotic resistance genes, and linkages with CRISPR-Cas systems. *mSystems* 6:e0121120. doi: 10.1128/mSystems.01211-20
- Qin, Q., Yan, S., Yang, Y., Chen, J., Li, T., Gao, X., et al. (2021). A Metagenome-wide association study of the gut microbiome and metabolic syndrome. *Front. Microbiol.* 12:682721. doi: 10.3389/fmicb.2021.682721
- Quan, Y., Song, K., Zhang, Y., Zhu, C., Shen, Z., Wu, S., et al. (2018). *Roseburia intestinalis*-derived flagellin is a negative regulator of intestinal inflammation. *Biochem. Biophys. Res. Commun.* 501, 791–799. doi: 10.1016/j.bbrc.2018.05.075
- Rastogi, S., Mittal, V., and Singh, A. (2020). In vitro evaluation of probiotic potential and safety assessment of *lactobacillus mucosae* strains isolated from Donkey's lactation. *Probiotics Antimicrob Proteins* 12, 1045–1056. doi: 10.1007/s12602-019-09610-0
- Ren, M., Li, H., Fu, Z., and Li, Q. (2021). Succession analysis of gut microbiota structure of participants from long-lived families in Hechi, Guangxi, China. *Microorganisms* 9:2524. doi: 10.3390/microorganisms9122524
- Reuben, R. C., Roy, P. C., Sarkar, S. L., Rubayet Ul Alam, A. S. M., and Jahid, I. K. (2020). Characterization and evaluation of lactic acid bacteria from indigenous raw milk for potential probiotic properties. *J. Dairy Sci.* 103, 1223–1237. doi: 10.3168/jds.2019-17092
- Rocha-Mendoza, D., Kosmerl, E., Miyagusuku-Cruzado, G., Giusti, M. M., Jiménez-Flores, R., and García-Cano, I. (2020). Growth of lactic acid bacteria in milk phospholipids enhances their adhesion to Caco-2 cells. *J. Dairy Sci.* 103, 7707–7718. doi: 10.3168/jds.2020-18277
- Rodriguez, J., Hiel, S., Neyrinck, A. M., Le Roy, T., Pötgens, S. A., Leyrolle, Q., et al. (2020). Discovery of the gut microbial signature driving the efficacy of prebiotic intervention in obese patients. *Gut* 69, 1975–1987. doi: 10.1093/gut/jgaa319
- Salminen, S., Collado, M. C., Endo, A., Hill, C., Lebeer, S., Quigley, E. M. M., et al. (2021). The international scientific Association of Probiotics and Prebiotics (ISAPP) consensus statement on the definition and scope of postbiotics. *Nat. Rev. Gastroenterol. Hepatol.* 18, 649–667. doi: 10.1038/s41575-021-00440-6
- Schäffler, H., Herlemann, D. P., Klinzke, P., Berlin, P., Kreikemeyer, B., Jaster, R., et al. (2018). Vitamin D administration leads to a shift of the intestinal bacterial composition in Crohn's disease patients, but not in healthy controls. *J. Dig. Dis.* 19, 225–234. doi: 10.1111/1751-2980.12591
- Seddik, H. A., Bendali, E., Gancel, F., Fliss, I., Spano, G., and Drider, D. (2017). *Lactobacillus plantarum* and its probiotic and food potentialities. *Probiotics Antimicrob Proteins* 9, 111–122. doi: 10.1007/s12602-017-9264-z
- Segain, J. P., Raingeard de la Blétière, D., Bourreille, A., Leray, V., Gervois, N., Rosales, C., et al. (2000). Butyrate inhibits inflammatory responses through NFκB inhibition: implications for Crohn's disease. *Gut* 47, 397–403. doi: 10.1136/gut.47.3.397
- Seo, B., Jeon, K., Moon, S., Lee, K., Kim, W. K., Jeong, H., et al. (2020). *Roseburia spp.* abundance associates with alcohol consumption in humans and its administration ameliorates alcoholic fatty liver in mice. *Cell Host Microbe* 27, 25–40.e6. doi: 10.1016/j.chom.2019.11.001
- Sharma, K., Attri, S., and Goel, G. (2019). Selection and evaluation of probiotic and functional characteristics of autochthonous lactic acid bacteria isolated from fermented wheat flour dough Babroo. *Probiotics Antimicrob Proteins* 11, 774–784. doi: 10.1007/s12602-018-9466-z
- Shen, Z., Zhu, C., Quan, Y., Yang, J., Yuan, W., Yang, Z., et al. (2018). Insights into *Roseburia intestinalis* which alleviates experimental colitis pathology by inducing anti-inflammatory responses. *J. Gastroenterol. Hepatol.* 33, 1751–1760. doi: 10.1111/jgh.14144
- Solieri, L., Bianchi, A., Mottolese, G., Lemmetti, F., and Giudici, P. (2014). Tailoring the probiotic potential of non-starter *lactobacillus* strains from ripened

- Parmigiano Reggiano cheese by in vitro screening and principal component analysis. *Food Microbiol.* 38, 240–249. doi: 10.1016/j.fm.2013.10.003
- Sonnenburg, J. L., Angenent, L. T., and Gordon, J. I. (2004). Getting a grip on things: how do communities of bacterial symbionts become established in our intestine? *Nat. Immunol.* 5, 569–573. doi: 10.1038/ni1079
- Steppe, M., Van Nieuwerburgh, F., Vercauteren, G., Boyen, F., Eeckhaut, V., Deforce, D., et al. (2014). Safety assessment of the butyrate-producing *Butyrivibrio pullicaecorum* strain 25-3(T), a potential probiotic for patients with inflammatory bowel disease, based on oral toxicity tests and whole genome sequencing. *Food Chem. Toxicol.* 72, 129–137. doi: 10.1016/j.fct.2014.06.024
- Sun, Z., Harris, H. M., McCann, A., Guo, C., Argimón, S., Zhang, W., et al. (2015). Expanding the biotechnology potential of lactobacilli through comparative genomics of 213 strains and associated genera. *Nat. Commun.* 6, 8322. doi: 10.1038/ncomms9322
- Tavella, T., Rampelli, S., Guidarelli, G., Bazzocchi, A., Gasperini, C., Pujos-Guillot, E., et al. (2021). Elevated gut microbiome abundance of Christensenellaceae, Porphyromonadaceae and Rikenellaceae is associated with reduced visceral adipose tissue and healthier metabolic profile in Italian elderly. *Gut Microbes* 13, 1–19. doi: 10.1080/1949076.2021.1880221
- Ubeda, C., Bucci, V., Caballero, S., Djukovic, A., Toussaint, N. C., Equinda, M., et al. (2013). Intestinal microbiota containing *Barnesiella* species cures vancomycin-resistant *enterococcus faecium* colonization. *Infect. Immun.* 81, 965–973. doi: 10.1128/IAI.01197-12
- Van den Abbeele, P., Belzer, C., Goossens, M., Kleerebezem, M., De Vos, W. M., Thas, O., et al. (2013). Butyrate-producing clostridium cluster XIVa species specifically colonize mucins in an in vitro gut model. *ISME J.* 7, 949–961. doi: 10.1038/ismej.2012.158
- van Heel, A. J., de Jong, A., Song, C., Viel, J. H., Kok, J., and Kuipers, O. P. (2018). BAGEL4: a user-friendly web server to thoroughly mine RiPPs and bacteriocins. *Nucleic Acids Res.* 46, W278–w281. doi: 10.1093/nar/gky383
- Vankerckhoven, V., Huys, G., Vancanneyt, M., Vael, C., Klare, I., Romond, M.-B., et al. (2008). Biosafety assessment of probiotics used for human consumption: recommendations from the EU-PROSAFE project. *Trends Food Sci. Technol.* 19, 102–114. doi: 10.1016/j.tifs.2007.07.013
- Vargas, L. A., Olson, D. W., and Aryana, K. J. (2015). Whey protein isolate improves acid and bile tolerances of *Streptococcus thermophilus* ST-M5 and *lactobacillus delbrueckii* ssp. *bulgaricus* LB-12. *J. Dairy Sci.* 98, 2215–2221. doi: 10.3168/jds.2014-8869
- Wang, G., Chen, Y., Fei, S., Xie, C., Xia, Y., and Ai, L. (2021). Colonisation with endogenous *lactobacillus reuteri* R28 and exogenous *lactobacillus plantarum* AR17-1 and the effects on intestinal inflammation in mice. *Food Funct.* 12, 2481–2488. doi: 10.1039/D0FO02624G
- Wang, G., Liu, Y., Lu, Z., Yang, Y., Xia, Y., Lai, P. F., et al. (2019). The ameliorative effect of a *lactobacillus* strain with good adhesion ability against dextran sulfate sodium-induced murine colitis. *Food Funct.* 10, 397–409. doi: 10.1039/C8FO01453A
- Wang, L., Si, W., Xue, H., and Zhao, X. (2017). A fibronectin-binding protein (FbpA) of *Weissella cibaria* inhibits colonization and infection of *Staphylococcus aureus* in mammary glands. *Cell. Microbiol.* 19:2731. doi: 10.1111/cmi.12731
- Weiss, G. A., Chassard, C., and Hennet, T. (2014). Selective proliferation of intestinal *Barnesiella* under fucosyllactose supplementation in mice. *Br. J. Nutr.* 111, 1602–1610. doi: 10.1017/S0007114513004200
- Wu, X., Pan, S., Luo, W., Shen, Z., Meng, X., Xiao, M., et al. (2020). *Roseburia intestinalis*-derived flagellin ameliorates colitis by targeting miR-223-3p-mediated activation of NLRP3 inflammasome and pyroptosis. *Mol. Med. Rep.* 22, 2695–2704. doi: 10.3892/mmr.2020.11351
- Xu, F., Cheng, Y., Ruan, G., Fan, L., Tian, Y., Xiao, Z., et al. (2021). New pathway ameliorating ulcerative colitis: focus on *Roseburia intestinalis* and the gut-brain axis. *Ther. Adv. Gastroenterol.* 14, 175628482110044. doi: 10.1177/17562848211004469
- Xu, X., Zhang, W., Guo, M., Xiao, C., Fu, Z., Yu, S., et al. (2022). Integrated analysis of gut microbiome and host immune responses in COVID-19. *Front. Med.* 16, 263–275. doi: 10.1007/s11684-022-0921-6
- Yadav, H., Lee, J. H., Lloyd, J., Walter, P., and Rane, S. G. (2013). Beneficial metabolic effects of a probiotic via butyrate-induced GLP-1 hormone secretion. *J. Biol. Chem.* 288, 25088–25097. doi: 10.1074/jbc.M113.452516
- Zhao, X., Zhao, C., Yang, L., Jiang, L., Zhang, J., Yu, X., et al. (2022). Spatial and temporal persistence of fluorescent *Lactiplantibacillus plantarum* RS-09 in intestinal tract. *Front. Microbiol.* 13:843650. doi: 10.3389/fmicb.2022.843650
- Zhou, W., Zhang, D., Li, Z., Jiang, H., Li, J., Ren, R., et al. (2021). The fecal microbiota of patients with pancreatic ductal adenocarcinoma and autoimmune pancreatitis characterized by metagenomic sequencing. *J. Transl. Med.* 19, 215. doi: 10.1186/s12967-021-02882-7
- Zhu, Y., Guo, L., and Yang, Q. (2020). Partial replacement of nitrite with a novel probiotic *lactobacillus plantarum* on nitrate, color, biogenic amines and gel properties of Chinese fermented sausages. *Food Res. Int.* 137:109351. doi: 10.1016/j.foodres.2020.109351
- Zhu, C., Song, K., Shen, Z., Quan, Y., Tan, B., Luo, W., et al. (2018). *Roseburia intestinalis* inhibits interleukin-17 excretion and promotes regulatory T cells differentiation in colitis. *Mol. Med. Rep.* 17, 7567–7574. doi: 10.3892/mmr.2018.8833
- Zmora, N., Zilberman-Schapira, G., Suez, J., Mor, U., Dori-Bachash, M., Bashirades, S., et al. (2018). Personalized gut mucosal colonization resistance to empiric probiotics is associated with unique host and microbiome features. *Cell* 174, 1388–1405.e21. doi: 10.1016/j.cell.2018.08.041